Molecular Biotechnology
https://doi.org/10.1007/s12033-023-00916-7

ORIGINAL PAPER

Identification of Cutinolytic Esterase from Microplastic-Associated Microbiota Using Functional Metagenomics and Its Plastic Degrading Potential

Ali Osman Adıgüzel[1] · Fatma Şen[1] · Serpil Könen-Adıgüzel[2] · Ahmet Erkan Kıdeyş[3] · Arzu Karahan[3] · Tuğrul Doruk[1] · Münir Tunçer[1]

Received: 11 August 2023 / Accepted: 19 September 2023

Abstract

Plastic pollution has threatened biodiversity and human health by shrinking habitats, reducing food quality, and limiting the activities of organisms. Therefore, global interest in discovering novel enzymes capable of degrading plastics has increased considerably. Within this context, the functional metagenomic approach, which allows for unlocking the functional potential of uncultivable microbial biodiversity, was used to discover a plastic-degrading enzyme. First, metagenomic libraries derived from microplastic-associated microbiota were screened for esterases capable of degrading both tributyrin and polycaprolactone. Clone KAD01 produced esterase highly active against *p*-nitrophenyl esters (C2–C16). The gene corresponding to the enzyme activity showed moderate identity (≤ 55.94%) to any known esterases/cutinases. The gene was extracellularly expressed with a 6× histidine tag in *E. coli* BL21(DE3), extracellularly. Titer of the enzyme (CEstKAD01) was raised from 21.32 to 35.17 U/mL by the statistical optimization of expression conditions and media components. CEstKAD01 was most active at pH 7.0 and 30 °C. It was noteworthy stable over a wide pH (6.0–10.0) and temperature (20–50 °C). The enzyme was active and stable in elevated NaCl concentrations up to 12% (w/v). Pre-incubation of CEstKAD01 with Mg^{2+}, Mn^{2+}, and Ca^{2+} increased the enzyme activity. CEstKAD01 displayed an excellent tolerance against various chemicals and solvents. It was determined that 1 mg of the enzyme caused the release of 5.39 ± 0.18 mM fatty acids from 1 g apple cutin in 120 min. K_m and V_{max} values of CEstKAD01 against *p*-nitrophenyl butyrate were calculated to be 1.48 mM and 20.37 µmol/min, respectively. The enzyme caused 6.94 ± 0.55, 8.71 ± 0.56, 7.47 ± 0.47, and 9.22 ± 0.18% of weight loss in polystyrene, high-density polyethylene, low-density polyethylene, and polyvinyl chloride after 30-day incubation. The scanning electron microscopy (SEM) analysis indicated the formation of holes and pits on the plastic surfaces supporting the degradation. In addition, the change in chemical structure in plastics treated with the enzyme was determined by Fourier Transform Infrared Spectroscopy (FTIR) analysis. Finally, the degradation products were found to have no genotoxic potential. To our knowledge, no cutinolytic esterase with the potential to degrade polystyrene (PS), high-density polyethylene (HDPE), low-density polyethylene (LDPE), and polyvinyl chloride (PVC) has been identified from metagenomes derived from microplastic-associated microbiota.

Keywords Functional metagenomic · Plastic degradation · Cutinolytic esterase · Expression · Characterization

✉ Ali Osman Adıgüzel
adiguzel.ali.osman@gmail.com

[1] Department of Molecular Biology and Genetics, Faculty of Science, Ondokuz Mayıs University, Samsun 55000, Turkey

[2] Department of Biology, Faculty of Science, Mersin University, Mersin, Turkey

[3] Department of Marine Biology and Fisheries, Institute of Marine Sciences, Middle East Technical University, Mersin, Turkey

Introduction

The word "plastic" originates from the Greek "plastikos," meaning "capable of taking different forms" [1]. Plastics are long-chain polymeric molecules derived from petroleum [2]. Industrial production of the first modern plastic developed in 1907 started in 1940 [3]. Today, plastics have become indispensable for daily life and many industries due to their easy formability, low cost, and resistance to harsh environmental conditions. It has been reported that plastic production,

Published online: 10 October 2023

1.5 million tons in the 1950s, will exceed 33 billion tons in 2050 [4]. About 74% of the raw plastic produced annually is waste, 9% of which is recycled, 12% incinerated, and the other 79% is stored in landfills or dumped directly into the environment. About 74% of annual raw plastic production becomes waste. Of the waste plastic, 9% undergoes recycling, 12% goes through incineration, and the remaining 79% is either disposed of in landfills or released into the environment [5]. Borrello et al. [6] estimated that 19 to 23 million metric tons of plastic waste was released into the aquatic ecosystem in 2016. Their barely degradable property in nature threatens ecosystems and the health of living things.

So far, two basic policies have been proposed to reduce plastic waste pollution. First, "less waste generation" has unfortunately not been realized due to the increasing population and changing consumption habits [7]. The markets have not adopted the policy of using bio-plastics instead of petroleum derivatives since bio-plastics produced from raw materials such as polylactic acid (PLA), polyhydroxybutyrate (PHB), and starch have various weaknesses, including brittle nature and short half-life [8]. Hence, plastic waste management (PWM) has gained the attention of many researchers in previous years. PWM consists of physical recovery, incineration, landfill, and biodegradation processes. Physical recycling, an easily applicable and cost-effective method, is designed to convert thermoplastics to molding plastics products by washing, hot extrusion, and grinding [9]. However, this method can be applied to only 5–10% of total global plastic waste [10]. Incineration increases the emission of toxic gases such as dioxins and furans, which cause endocrine and immune system disorders as well as different forms of cancer [11]. Landfilling plastics can result in the leakage of hazardous chemicals and the entry of microplastics into the food chain. On the other hand, biodegradation is an eco-friendly and low-cost process using microorganisms or enzymes [7]. Therefore, many researchers have focused on discovering biological agents involved in the degradation of plastics.

Polystyrene (PS), high-density polyethylene (HDPE), low-density polyethylene (LDPE), and polyvinyl chloride (PVC) are among the most preferred plastics on the market. Plastics Europa [12] announced that 5.3, 12.5, 14.4, and 12.9% of plastic produced in 2021 (390.7 Mt) consisted of PS-, HDPE-, LDPE-, and PVC-based polymers, respectively. PS, HDPE, LDPE, and PVC also constitute the majority of plastic waste. These polymers with high molecular weight are highly hydrophobic. In addition, the presence of highly stable C–C and C–H covalent bonds in their backbone and the absence of functional groups that can be easily oxidized/hydrolyzed on their surfaces make them resistant to biodegradation [13]. Previously, several studies have demonstrated their biodegradation by microorganisms. In addition, they showed that the extracellular enzymes of microorganisms could play a significant role in the degradation of plastics with a C–C backbone [10, 14–19]. However, limited reports in the literature describe the use of a specific enzyme for PS, HDPE, LDPE, or PVC degradation.

Esterases (EC.3.1.1.1.1) and cutinases (EC.3.1.1.74) belonging to the carboxylic ester hydrolases (EC.3.1.1.1.-) are the major enzymes responsible for the degradation of polyester-based plastics [20]. Both enzymes, classified in α/β hydrolase family, catalyze the cleavage of ester bonds of fatty acid esters [21, 22]. These enzymes, which are members of the serine hydrolase superfamily due to the serine in their catalytic triad (Ser-Asp/Glu-His), share the consensus Gly-X-Ser-X-Gly (X is any amino acid residue) pentapeptide sequence. They are distinguishable by their substrate specificity [23]. Esterases preferentially act on relatively short-chain fatty acids ($C < 10$), whereas cutinases can hydrolyze ester bonds in both short and long triglycerides. Unlike lipases, they are active not only at hydrophilic–hydrophobic interfaces but also in emulsified hydrophobic solutions.

The discovery of new enzymes fulfilling specific needs depends on the efficiency of the screening strategy and the diversity of candidate genes. In the traditional methods based on isolating microorganisms from different habitats, gene diversity remains quite limited, even if your scanning strategy is powerful, since it is well known that only about 1% of the bacteria in nature can be cultured with conventional isolation methods [24]. On the other hand, functional metagenomic methods offer the opportunity to benefit from the genomes of microorganisms that cannot be cultured. In the last decade, many enzymes have been discovered using a functional metagenomic approach [25, 26]. However, no reports identify a plastic-degrading enzyme from microplastic-associated microbiota using functional metagenomics.

Previous cultural and sequence-based metagenomic approaches have shown that plastics are newly emerged anthropogenic habitats (plastisphere) and host plastic-degrading microbial strains [27, 28]. Additionally, several metatranscriptomic and metaproteomic studies have demonstrated the role of lipolytic enzymes secreted from plastic-associated microorganisms in the degradation of plastics [29]. Within this context, we aimed to exploit this untapped genetic potential of plastic-associated microbiota to degrade plastics. Therefore, in the present study, a novel gene encoding a functional cutinolytic esterase was identified from fosmid libraries constructed with DNA extracted from microplastic-associated microbiota. The gene was cloned into pET20b(+) and expressed in *E. coli* BL21(DE3). Expression was optimized using response surface methodology (RSM). The expressed enzyme was purified and then characterized. Afterward, the potential of the enzyme to degrade PS, HDPE, LDPE, and PVC was determined. Finally, the genotoxicity of the degradation products was assessed.

Materials and Methods

Chemicals and Reagents

Low melting agarose (LMA) gel, substrates, solvents, phenylmethylsulfonyl fluoride (PMSF), 1,4-dithiothreitol (DTT), sodium dodecyl sulfate (SDS), β-mercaptoethanol (βME), acrylamide, bis-acrylamide, *p*-nitrophenyl acetate (*p*NP-A), *p*-nitrophenyl butyrate (*p*NP-B), *p*-nitrophenyl caprylate (*p*NP-C), *p*-nitrophenyl laurate (*p*NP-L), *p*-nitrophenyl myristate (*p*NP-M), *p*-nitrophenyl palmitate (*p*NP-P), polycaprolactone (PCL), tributyrin (TR), ethylenediaminetetraacetic acid (EDTA), and proteinase K were purchased from Sigma-Aldrich (Darmstadt, Germany). Buffers and media components were procured from Merck (Darmstadt, Germany). *P*-nitrophenyl hexanoate (*p*NP-H) was purchased from Şahinler Kimya (İstanbul, Turkey). Petri dishes and glass materials were obtained from Isolab (Eschau, Germany). Restriction enzymes were procured from Thermo Fisher Scientific (Waltham, MA). Ni-NTA Rezin was obtained from QIAGEN (Hilden, Germany). Other chemicals and reagents were purchased from Panreac Applichem (Darmstadt, Germany), Tekkim (Bursa, Turkey), Condolab (Madrid, Spain), or HiMedia (Mumbai, India).

Bacterial Strains and Plasmids

E. coli EPI300-T1^R host cell and pCC2FOS™ fosmid vector in CopyControl™ http Fosmid Library Production Kit (Lucigen, a part of LGC Biosearch Technologies, Middleton, WI, USA) were used for cloning of metagenomic DNA. *E. coli* DH5α cell (Thermo Fisher Scientific™, Waltham, MA, USA) and pUC19 plasmid (NEB, Ipswich, MA, USA) were employed as host and vector in subcloning and secondary screening studies, respectively. *E. coli* BL21 (DE3) competent cell (Thermo Fisher Scientific) and pET20b(+) plasmid vector (Novagen, Madison, WI, USA) were used for heterologous protein expression. *E. coli* strains were maintained on Luria Bertani (LB) agar (10 g/L peptone, 5 g/L yeast extract, 10 g/L NaCl, and 12 g/L agar) and cultured in LB broth supplemented with appropriate antibiotics (chloramphenicol, ampicillin, and kanamycin) and mineral ($MgSO_4$) [30].

Microplastic Sample Collection

Plastic pieces were collected from the tidal zone of 12 beaches in January 2021 in Turkey. The locations of these beaches, which have high-population cities nearby and are visited by many tourists throughout the year, are shown in Fig. 1. Samples were taken from sands at a depth of 5–20 cm. Sampling was performed from ten different sites

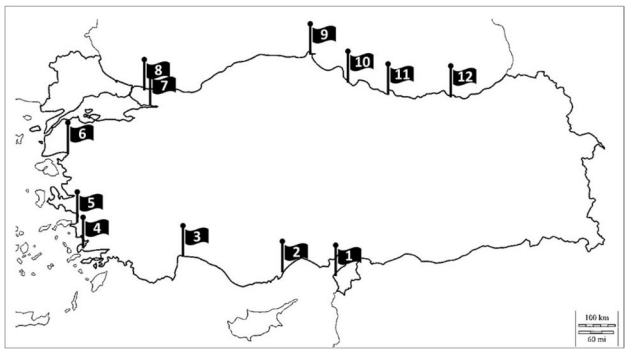

Fig. 1 Sampling locations; **1** Çevlik Beach in Samandağı/Hatay (lat. 32° 12′ N and long. 35° 92′ E), **2** Maidens Tower Sea Castle Beach in Erdemli/Mersin (lat. 36° 46′ N and long. 34° 14′ E), **3** Konyaaltı Beach in Konyaaltı/Antalya (lat. 36° 86′ N and long. 30° 63′ E), **4** Gümbet Beach in Bodrum/Muğla (lat. 37° 03′ N and long. 27° 40′ E), **5** Ladies Beach in Kuşadası/Aydın (lat. 37° 84′ N and long. 27° 24′ E), **6** Altınkum Beach in Edremit/Balıkesir (lat. 39° 57′ N and long. 26° 94′ E), **7** Bayramoğlu Ada Beach in Gebze/Kocaeli (lat. 40° 79′ N and long. 29° 33′ E), **8** Şile Beach in Şile/İstanbul (lat. 41° 17′ N and long. 29° 59′ E), **9** Akliman Beach in Sinop (lat. 42° 02′ N and long. 35° 06′ E), **10** Atakum Beach in Atakum/Samsun (lat. 31° 33′ N and long. 36° 28′ E), **11** Bolaman Beach in Fatsa/Ordu (lat. 41° 03′ N and long. 37° 59′ E), **12** Kaşüstü Beach in Yomra/Trabzon (lat. 40° 96′ N and long. 39° 84′ E)

(1 m^2) at equal distances in each location. Picked samples were transferred to sterile 50-mL falcon tubes and transported to the laboratory in a cold chain bag containing ice. They were then stored at + 4 °C until the metagenomic DNA extraction study.

DNA Extraction from Plastic-Associated Microbiota

A total of 40 microplastic pieces (0.1–5 mm) from each location were transferred to new sterile 50-mL falcon tubes from each location and were subjected to DNA extraction performed by the modified phenol–chloroform method [31]. Briefly, the sample was mixed with 5 mL of lysis buffer (1 mM Tris HCl supplemented with 25 mM Na_2EDTA, %1 SDS, and 100 mM NaCl; pH 8.0) and 50 µL of proteinase K solution (100 U/µL). The mixture was incubated at 50 °C for 30 min. Then, 100 µL of lysozyme solution was pipetted into the tube. After incubation at 37 °C for 30 min, 2 g of zirconium beads was transferred to the tube. After incubation at 37 °C for 30 min, the mixture was vortexed for 10 min in the presence of zirconium beads. Next, 5 mL of phenol was added to the mixture. The supernatant collected after centrifugation at 45,000×*g* for 10 min was mixed with 5 mL of phenol–chloroform–isoamyl alcohol (25:24:1). The DNA in the aqueous phase of centrifuged (4500×*g*, 10 min) mixture was precipitated with two volumes of absolute ethanol and 1 volume of 5 M NaCl. Recovered DNA with centrifugation

was air dried, washed with 70% (v/v) ethanol, and dissolved in 1X TE buffer.

Metagenomic Library Construction

Extracted DNAs were randomly fragmented by vigorous pipetting. Fragments were separated on 1% LMA gel (25 × 25 cm) overnight at a constant voltage of 30 V using a Sub-Cell Model 192 horizontal electrophoresis system (Bio-rad Laboratories, Hercules, CA). DNA fragments of 30–40 kb blunted and 5′-phosphorylated by end-repairing after being retrieved by GeneJET gel extraction kit (Thermo Scientific™, Waltham, MA, USA) in line with the manufacturer's recommendations. The prepared DNA fragments were ligated to pCC2FOS™ fosmids by Fast-Link DNA Ligase in the presence of 1 mM ATP as described in the protocol of CopyControl™ HTTP Fosmid Library Production Kit. Recombinant DNA molecules were introduced into *E. coli* EPI300™-T1^{R} cells after being packaged into phage particles following the same protocol. Afterward, clones that can grow on LB agar supplemented with 12.5 µg/mL chloramphenicol were subjected to further screening study [30].

Functional Screening of Libraries

The cutinolytic esterase activity of metagenomic clones was screened using Tributyrin-LB (TrLB; LB medium, 12.5 µg/mL chloramphenicol, 2 µL/mL auto-induction solution, and 10 µL/mL tributyrin) agar and polycaprolactone-LB (PcLB; 12.5 µg/mL chloramphenicol, 2 µL/mL auto-induction solution, and 1 µg/mL polycaprolactone) agar medium [22]. Metagenomic clones were individually spot inoculated on both media using a sterile toothpick. Plates were incubated at 37 °C for 24 h. A clear zone around the growing colonies on both TrLB and PcLB agar plates indicated cutinolytic enzyme production. Positive metagenomics clones were grown in LB broth supplemented with chloramphenicol and auto-induction solution. Then, intracellular and extracellular crude enzyme solutions of positive metagenomic clones were further tested for the ability to hydrolyze *p*NP-B, *p*NP-A, *p*NP-H, *p*NP-C, *p*NP-L, *p*NP-M, and *p*NP-P.

Subcloning and Sequence Analysis

The fosmid and pUC19 plasmid, extracted and purified using the QIAprep Spin Miniprep kit from the selected metagenomic clone and *E. coli* DH5α cells, respectively, were digested with SmaI (Thermo Scientific, Waltham, MA, USA). Digestion was performed using 10 U of enzyme per 0.5 µg of DNA for 2 h at 30 °C. Each 50 ng of linearized pUC19 was incubated with 100 ng of the fosmid DNA fragments (2–6 kb) in 50 mM Tris–HCl buffer (pH 7.5) containing 10 mM $MgCl_2$, 10 mM DTT, 1 mM ATP, and 1 U T4 DNA ligase for 4 h at 22 °C. Plasmids in the resulting ligation mixture were introduced into chemically competent *E. coli* DH5α cells through heat shock. Transformants carrying the recombinant plasmids were determined through blue/white selection and screened using antibiotic-free TrLB and PcLB with IPTG instead of the auto-induction solution.

Insert from the clone, capable of degrading both TRB and PCL, was sequenced (BM Labosis, Ankara, Turkey) using universal M13 forward (5′-CGCCAGGGTTTTCCC AGTCACGAC-3′) and M13 reverse (5′-CAGGAAACA GCTATGAC-3′) primers. Open reading frame (ORF) was predicted using an online server tool Open Reading Frame (ORF) Finder (https://www.ncbi.nlm.nih.gov/orffinder/) [32]. The DNA sequences of the gene were converted to amino acid sequences for bioinformatics analysis of the corresponding enzyme. The most likely function and classification of the enzyme were searched based on the HMMER algorithm using the PFAM database [33]. The similarity between the amino acid sequences of the enzyme and its functional homologs was identified using Blastp [34]. Physicochemical properties of the protein were computed via the Expasy ProtoParam tool (https://web.expasy.org/protparam/). Sequences were aligned using Clustal W (https://www.genome.jp/tools-bin/clustalw) according to the MUSCLE algorithm and then visualized using Jalview 2.11.2.0 [35]. The phylogenetic tree showing the evolutionary relationship between the enzyme and its functional homologs was generated by the neighbor-joining method using MEGA X software [36]. The secondary structure of the protein was assessed using "Sequence Annotated by Structure (SAS)" [37], PSIPRED (http://bioinf.cs.ucl.ac.uk/), and Phyre^2 [38] web servers. The protein's three-dimensional (3D) structure was predicted using the SWISS-MODEL tool [39].

Heterologous Expression and Purification

The gene was amplified through polymerase chain reaction (PCR) using forward and reverse primers with the BamHI restriction site. PCR product, purified using FavorPrep PCR Clean-Up Kit (Favorgen) according to the manufacturer's instruction, and pET20b(+) were digested with BamHI restriction enzyme at 37 °C for 2 h. Ligation and transformation were performed following the protocol mentioned above. *E. coli* BL21(DE3) harboring the recombinant plasmid, confirmed previously by the colony PCR using the gene primers, cultivated in LB medium with ampicillin at 37 °C and 200 rpm until the OD_{600} of the culture reaches 0.6. Subsequently, the expression was induced by adding IPTG at a final concentration of 0.125 mM. The culture was further incubated for 16 h under the same condition. Extracellular crude enzyme solutions were passed through the Ni-NTA resin equilibrated with 50 mM Tris HCl containing 500 mM NaCl, 10 mM imidazole, and 10% (v/v) glycerol. Binding

proteins were eluted with 50–500 mM imidazole gradient. Fractions in which enzyme activity was detected were pooled, concentrated, and dialyzed against 50 mM phosphate buffer (pH 7.0) for further studies. Expression and purification were analyzed with SDS-PAGE [40].

Preparation of Intracellular and Extracellular Crude Enzyme Solutions

The culture was centrifuged (10,000×*g*) at 4 °C for 10 min. The supernatant was used as an extracellular crude enzyme solution. On the other hand, collected cells were lysed by sonication in 20 mM Tris–HCl buffer containing 100 mM NaCl, 1 mM EDTA, 0.1% Triton X-100, and 5 mM CHAPS. The lysate was used as an intracellular crude enzyme solution.

Enzyme Assay and Determination of Protein Concentration

The enzyme assays were carried out as described by Adıgüzel [22]. Total protein concentration was determined using the Bradford method [41].

Biochemical Characterization

Enzyme assays were performed using *p*NP-B in all characterization studies. The effect of the pH was assessed by measuring the enzyme activity at different pHs using acetate (pH 4.0–6.0), phosphate (pH 6.0–7.0), Tris–HCl (pH 7.0–9.0), and Glycine–NaOH (pH 8.0–10.0) buffer systems. The influence of the temperature was determined by conducting enzyme assays in various temperatures (20–60 °C). The thermal stability of the enzyme was determined by pre-incubating the enzyme at 50 and 60 °C for 60–240 min and measuring its residual activity at 30 min intervals. The pH stability was assessed by 1 h pre-incubation of the enzyme in different pHs.

The effect of NaCl was studied by assaying the enzyme activity in the presence of NaCl at different concentrations up to 12%. The enzyme was pre-incubated substrate-free reaction mixture including varying concentrations of NaCl (3–12%) for 300 min, and subsequently, the remaining activity was determined by comparing it with the activity of the enzyme in the NaCl- and substrate-free reaction mixture pre-incubated under the same conditions.

The effect of various metal ions and chemicals on the stability was tested by incubating the enzyme for 60 min at 30 °C in the presence of Cu^{2+}, K^{+}, Mg^{2+}, Hg^{2+}, Zn^{2+}, Mn^{2+}, Li^{+}, Ca^{2+}, EDTA, dithiothreitol (DTT), SDS, biotin, and phenylmethylsulfonyl fluoride (PMSF) at final concentrations of 1 mM and 10 mM. To evaluate the stability of the enzyme against protease, the enzyme was incubated with proteinase K (5–30 U/mg protein) for 60 min at 30 °C. Afterward, the residual activity was determined by comparing the activity of the enzyme pre-incubated under the same conditions without any additives. The effect of various solvents (20%), such as ethanol, isopropanol, chloroform, DMSO, benzene, methanol, and acetone, on the enzyme stability was also evaluated similarly.

Cutin hydrolysis ability was assessed by incubating the enzyme in 1% cutin suspension prepared with 50 mM Tris–HCl buffer (pH 7.0) at 30 °C for 180 min. The concentration of releasing free fatty acids was determined by titration at regular intervals [42]. Cutin used in the study was extracted from apples, according to Chaudhari and Singhal [43].

Kinetic parameters were determined from the Lineweaver–Burk reciprocal plot drawn with the enzyme activity measured under optimum conditions in the presence of different concentrations of *p*NP-B.

Plastic Degradability Potential

Plastics including polystyrene (PS), low-density polyethylene (LDPE), high-density polyethylene (HDPE), polyethylene terephthalate (PET), polypropylene (PP), polystyrene (PS), and polyvinyl chloride (PVC) were cut into 0.5 cm^2 of pieces. Pieces were cleaned by incubation separately in Triton X 100 (5 g/L), 100 mM Na_2CO_3, and distilled water for 30 min and then dried until the weight remained constant [44]. They were subjected to enzymatic degradation after being sterilized with 95% ethanol. Degradation of PS (16.6 g/L), LDPE (18.1 g/L), HDPE (45.30 g/L), and PVC (93 g/L) was performed in 50 mM phosphate buffer (pH 7.0) containing the enzyme (1 U/mL) at 30 °C for 30 days. The enzyme solution was refreshed at 3-day regular intervals. At the end of the reaction, the pieces were cleaned as mentioned above and dried. Weight losses in plastic pieces were calculated as percentages. Their surface structures were examined using a Field Emission Scanning Electron Microscope (FESEM) (Zeiss-Supra 55, Oberkochen, Germany). In addition, Fourier Transform Infrared Spectroscopy (FTIR) spectra of the clean plastic pieces were recorded over the wavelength range 650–4000 cm^{-1} using a PerkinElmer® Spectrum™ 100 FTIR spectrometer (Germany) operating in ATR mode with a resolution of 4 cm^{-1}. Pieces incubated in enzyme-free buffer under the same condition were used as control.

Genotoxicity of Degradation Products

Saccharomyces cerevisiae cells, growth in Yeast Peptone Dextrose (YPD) medium at 32 °C and 200 rpm for 16 h, were used in experiments performed to assess the genotoxicity of degradation products. After enzymatic degradation,

plastic pieces were removed from the reaction mixture. Then, the reaction mixture was filter-sterilized. Finally, 10^6 cells were exposed to the reaction mixture for 3 h at 32 °C and 200 rpm. The reaction mixture from the control of degradation experiment was used as a negative control of the genotoxicity experiments, while 50 mM phosphate buffer containing H_2O_2 (50 µM) was used as a positive control. After exposure, yeast cells were subjected to the alkaline Comet Assay carried out according to Adiguzel et al. [45].

Statistical Analysis

Statistical significance ($p < 0.05$) of the results of the biochemical characterization and plastic degradation potential experiments was evaluated with a one-way ANOVA test using the XL Toolbox NG (https://www.xltoolbox.net/) tool integrated into Microsoft Excel Software. The statistical analyses of optimization studies were done using the Design Expert 7 software.

Results and Discussion

The most critical step in function-based metagenomic studies is DNA isolation. The isolated DNA should represent all cells in the sample but must be of high quality and sufficient quantity for library construction. The concentration and A260/280 ratio of DNA isolated from microplastics collected from each sampling location, which were determined with the help of the µDrop plate integrated into the microplate reader (Thermo Scientific, Multiskan GO, Waltham, MA, USA), ranged from 370 to 1448 ng/µL and from 1.79 to 2.05, respectively (Supplementary Materials 1 and 2). In addition, 16S rRNA genes in isolated DNA samples were amplified by polymerase chain reaction using 27f and 1496r universal primers. Thus, the presence of bacterial DNAs was verified. Agarose gel electrophoresis analysis of isolated DNA and 16S rRNA genes is shown in Supplementary Material 3a and Supplementary Material 3b, respectively. Metagenomic libraries were constructed from the fragmented DNAs (Supplementary Material 3c) with lengths ranging from 30 to 40 kb.

Approximately 50,000 clones were screened from the constructed libraries for each location. As a result of functional screening using TrLB and PcLB (Supplementary Material 4), it was observed that 184 and 30 metagenomic clones were able to degrade tributyrin and polycaprolactone, respectively. Among these, 24 were able to degrade both tributyrin and polycaprolactone. The hit rates of metagenomic clones degraded "tributyrin," "polycaprolactone," and "both tributyrin and polycaprolactone" were ~ 1/3261, 1/20,000, and 1/25,000, respectively. Similar to previous studies, the frequency of genes encoding esterolytic or cutinolytic enzymes was less than others. Sulaiman et al. [46] determined that only 1 of 6000 compost metagenomic library clones could degrade PET. Qiu et al. [47] reported that 14 among 9.7×10^4 clones in the lotus pond sludge metagenomic library caused the clear zone on LB agar plates containing tributyrin. In a study by Park et al. [48], in which esterase activity was screened in compost metagenomic library clones, 11 of 13,000 clones had a hydrolytic effect on tributyrin. In another study, Yan et al. [49] detected 9 clones that can be degrading tributyrin in the soil metagenomic library containing approximately 60,000 clones.

Cutinolytic esterases or cutinases can hydrolyze many substrates, such as soluble fatty acid esters, triglycerides, and insoluble polymers. Unlike lipases, they exhibit a higher affinity for pNP esters with a carbon chain shorter than C_8. In addition, most reports have shown that they have the most catalytic action against *p*NP-B among the *p*NP esters [21, 50, 51]. Therefore, the substrate specificity of the intracellular and extracellular crude enzyme solutions from positive metagenomic clones was determined (Supplementary Materials 5 and 6). Among them, crude enzyme solutions from the clone KAD01 exhibited maximum catalytic activity against *p*NP-B. It also showed a relatively high hydrolytic effect on the other *p*NP esters.

DNA pieces from digested fosmid of clone KAD01 were ligated onto pUC18 and transformed into DH5α host cells. Inserted fragment to vector in the transformant, which showed the enzyme activity, was sequenced. The predicted ORF (Supplementary Materials 7) with 1431 bp length encodes a protein (CEstKAD01) with 475 amino acid residues. Signal P analysis revealed the ORF does not contain any N-terminal signal sequence. The result indicated that CEstKAD01 could be an intracellular esterase like most others. According to the Expasy ProtParam tool, theoretical p*I*, aliphatic index, and grand average of hydropathicity (GRAVY) values are 5.15, 68.68, and −0.221, respectively. The tool also classifies CEstKAD01 as stable with a 35.15 instability index. Pfam analysis revealed that the enzyme is related to the alpha/beta hydrolase superfamily and carboxylesterases family (EC 3.1.1.X). Blastp analysis showed that it shares 55.94% amino acid similarity with the para-nitrobenzyl esterase from *Bacillus subtilis* (QHM13991.1). CEstKAD01 has 51.24 and 46.19% sequence identity with carboxylesterase family proteins from *Halopseudomonas oceani* (WP_104737618.1) and *Halopseudomonas aestusnigri* (WP_160003159.1). In addition, the amino acid sequence of CEstKAD01 displays 41.88 and 41.53% identity with those of sequences from *Thermobifida cellulosilytica* (E9LVH9.1) and *Saccharomonospora viridis* (WP_015787089.1) cutinases. The phylogenetic neighbor-joining tree consists of CEstKAD01 and various proteins shown in Fig. 2. In addition, the multiple sequence alignment of CEstKAD01 and other proteins used for constructing the

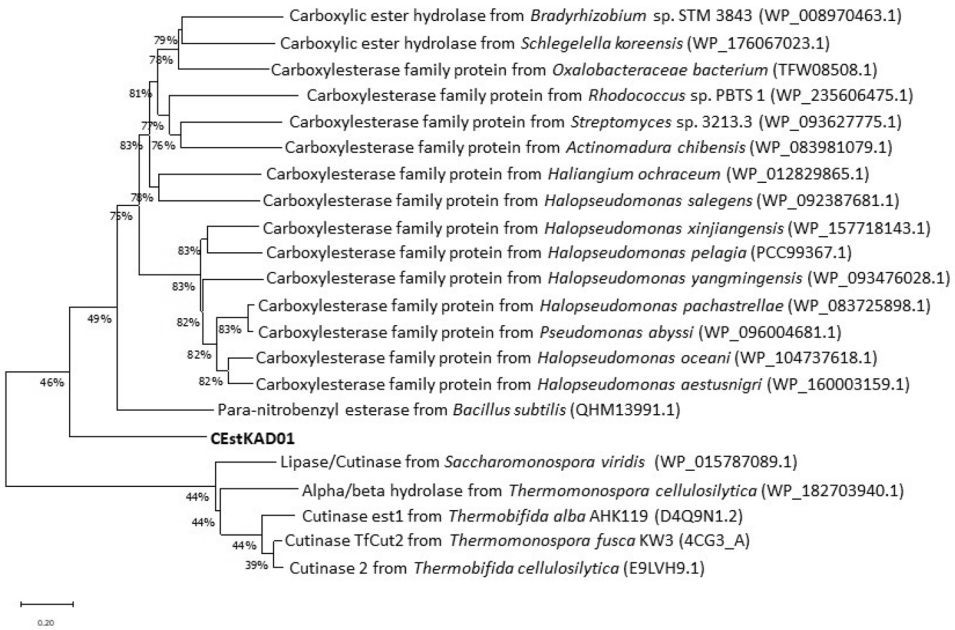

Fig. 2 The phylogenetic neighbor-joining tree of CEstKAD01 along with its close homologous. The numbers at the nodes describe the bootstrap confidence level percentage of 1000 copies. Similarity of CEstKAD01 in the amino acid level with carboxylesterase family proteins from *B. subtilis*, *H. oceani*, *H. aestusnigri*, *H. pachastrellae*, *P. abyssi*, *T. cellulosilytica*, *S. viridis*, *H. xinjiangensis*, *H. yangmingensis*, *S. koreensis*, *H. pelagia*, *A. chibensis*, *H. salegens*, *T. cellulosilytica*, *H. ochraceum*, *Rhodococcus* sp. PBTS 1, *Bradyrhizobium* sp. STM 3843, *O. bacterium*, *Streptomyces* sp. 3213.3, *T. alba* AHK119 and *T. fusca* KW3 are 55.94, 51.24, 46.19, 42.94, 42.23, 41.88, 41.53, 41.05, 38.61, 36.20, 35.55, 35.15, 34.34, 30.77, 30.24, 29.64, 29.23, 28.88, 27.54, 27.41, and 26.88%, respectively

phylogenetic tree was displayed in Supplementary Material 8. It showed that the S amino acid in the catalytic triad of CEstKAD01 is located within the conserved GXSXG amino acid motif, similar to other esterases and cutinases.

As illustrated in Fig. 3a, analyses on the secondary structure of CEstKAD01 showed that the enzyme contained more alpha helix than beta-sheet. According to the analysis of Phyre[2], 10% and 32% of the amino acid residues of CEstKAD01 are located in the beta-strand and alpha helix, respectively. PSIPRED analysis indicated that the enzyme includes three domains with boundaries located in the 111th and 265th amino acids. The 3D structure of CEstKAD01 was constructed with a template (A0A2D5N0C7.1.A, Carboxylic ester hydrolase from *Pseudomonadales* sp.) retrieved from Protein Data Bank (PDB) using SWISS-MODEL (Fig. 3b). CEstKAD01-target sequence similarity and identity values, calculated without considering the gaps, were found to be 0.56 and 82.40%, respectively. The Global Model Quality Estimate (GMQE) value for the constructed model was 0.91, indicating that the model was relatively high quality. From

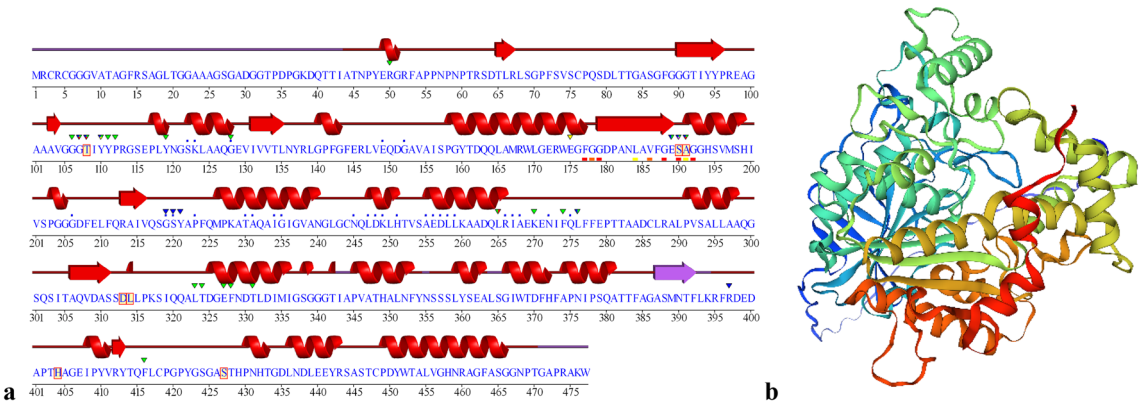

Fig. 3 **a** CEstKAD01's secondary structure predicted by SAS. **b** Three-dimensional structure of CEstKAD01 plotted by SWISS-MODEL

the constructed 3D structure, CEstKAD01 was estimated to be a monomer. Consistent with the secondary structure analysis, the structure of CEstKAD01 consisted of three α/β domains. In addition, solvent accessible surface area and volume of the model were predicted to be 2555.265 Å2 and 12,670.570 Å3, respectively.

Heterologous Expression and Purification of CEstKAD01

Briefly, 1425 bp of the gene was cloned into pET20b(+), and then the resultant construct was transformed into the *E. coli* BL21 (DE3). *E. coli* with pET20b(+) plasmid [*E. coli*-pET20b(+)] and *E. coli* with the recombinant plasmid [*E. coli*-pET20b(+)-CEstKAD01] were cultured in the absence and presence of IPTG. Their extracellular protein profiles were analyzed by SDS-PAGE (Fig. 4a). A distinct protein band with a molecular weight of about 50 kDa in the extracellular proteins of *E. coli*-pET20b-CEstKAD01 cultured in the presence of IPTG indicated that CEstKAD01 was successfully expressed heterologously. In addition, expression was verified by determining the tributyrin and PCL degradation ability of *E. coli*-pET20b(+)-CEstKAD01 on TrLB-agar and PcLB-agar (Supplementary Material 9). The expression conditions and media components were statistically optimized with a preliminary study to improve CEstKAD01 secretion (Supplementary Materials 10–12). Thus, the esterase titer was raised from 21.32 U/mL ± 1.01 to 35.17 ± 2.37 U/mL. Extracellular total protein concentration was estimated to be 0.395 ± 0.03 mg/mL and 0.42 ± 0.02 mg/mL under un-optimized and optimized condition, respectively. CEstKAD01 was purified 41.64-fold by eluting proteins bound to Ni-NTA resin using 400 mM imidazole solution (Fig. 4b). The molecular weight of the enzyme, purified with a final yield of 9.91%, was about 50 kDa, higher than previously reported many esterases and cutinases [52, 53].

Biochemical Characterization of CEstKAD01

CEstKAD01 was highly active in the pH range of 6–10, and showed maximum activity at pH 7 (Fig. 5a). The relative activity of CEstKAD01 was 43.03 ± 3.01 and 16.70 ± 1.86% at pH 5.0 and 4.0, respectively. The enzyme exhibited similar behavior in buffers Tris–HCl and glycine–NaOH buffer systems. On the other hand, it was observed that the catalytic activity of CEstKAD01 decreased in the acetate and phosphate buffer systems due to the kosmotropic and chaotropic impacts of ions. A similar optimal pH has been reported for esterases from compost [54] and cow rumen metagenomes [55]. Unlike the CEstKAD01, many esterases discovered by the functional metagenomic exhibited high activity only at alkali condition [56–58]. The ability of CEstKAD01 to demonstrate high activity under mild acidic to alkaline conditions makes it preferable for bioremediation applications.

The effect of temperature on CEstKAD01 is shown in Fig. 5b. The optimum temperature of CEstKAD01 was 30 °C similar to previously reported metagenome-derived esterases EstM-N2 [59], pl2ss [60], Est8 [61], hAGEst [62], PMGL3 [63], and Tan410 [64]. It retained over 90% of its maximum activity at 20, 25, 35, and 40 °C. In contrast, the catalytic activities of many other mesophilic metagenome-derived esterases and cutinases decrease dramatically below 30 °C [47, 55, 65]. The relative activity of CEstKAD01 at 45 and 50 °C was 79.31 ± 2.45 and 65.12 ± 1.33, respectively. However, increasing the assay temperature above 50 °C resulted in a significant decline in enzyme activity. The results showed that the enzyme could be tremendously valuable for environmental biotechnology applications in many aquatic and terrestrial habitats.

As shown in Fig. 6a, CEstKAD01 displayed stability over a broad pH range from 6.0 to 10.0, which was similar to Tan410 esterase from a soil metagenomics library [64], Est 6 from an activated sludge metagenome [66]. It preserved

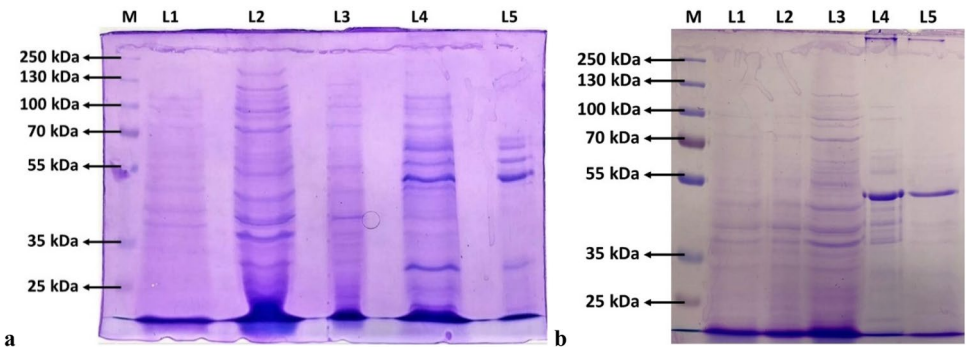

Fig. 4 **a** SDS-PAGE analysis shows extracellular protein profile of *E. coli*-pET20b(+) in the absence of IPTG (L1), *E. coli*-pET20b(+)-CEstKAD01 in the absence of IPTG (L2), *E. coli*-pET20b(+) in the presence of IPTG (L3), and *E. coli*-pET20b(+)-CEstKAD01 in the presence of IPTG (L4). **b** SDS-PAGE analysis of eluted proteins from Ni-NTA resin using 50 mM (L1), 100 mM (L2), 200 mM (L3), 300 mM (L4), and 400 mM (L5) imidazole solution

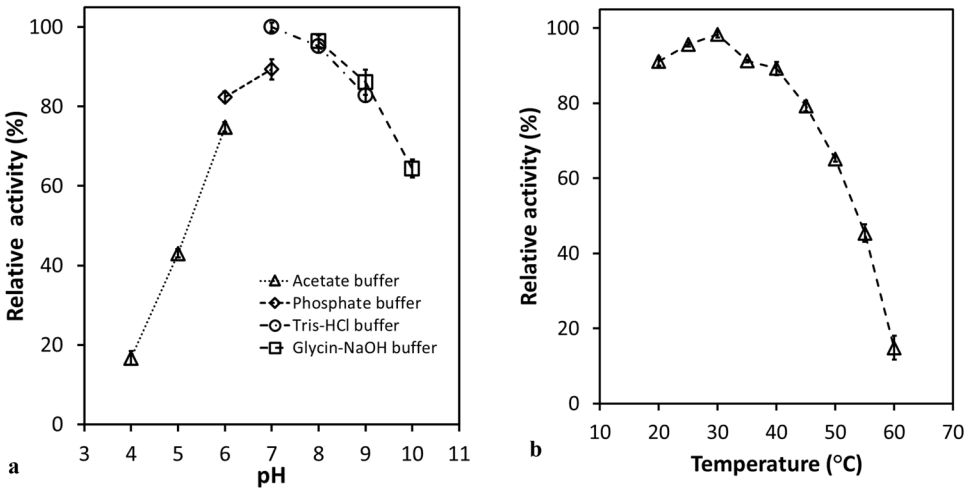

Fig. 5 **a** The influence of pH on the activity of CEstKAD01. Acetate (empty triangles), phosphate (empty diamonds), Tris–HCl (empty circles), and glycine–NaOH (empty squares) were used for adjust pH of the reaction mixture. **b** The effect of temperature on CEstKAD01 activity. The highest CEstKAD01 activity was accepted as 100% for each experimental set. Data from experiments with triplicate are presented with standard error bars

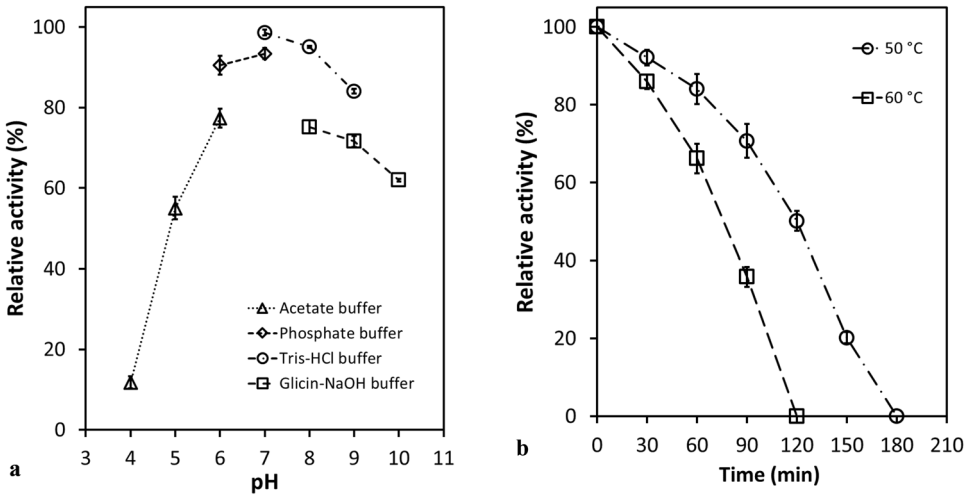

Fig. 6 **a** The relative activity of CEstKAD01 after pre-incubation at different pHs (4–10) for 60 min. Pre-incubation was performed in acetate (pH 4–6), phosphate (pH 6 and 7), tris–HCl (pH 7–9), and glycine–NaOH (pH 8–10) buffer systems. **b** The effect of temperature on CEstKAD01 stability. The enzyme was pre-incubated at 50 °C (empty circles) and 60 °C (empty squares) for 0–180 min. The initial activity of CEstKAD01 was accepted as 100% for each set of experiments. Data were shown with bars representing standard errors

98.65 ± 1.22, 95.09 ± 0.43, and 84.08 ± 1.01% of its initial activity at pH 7.0, 8.0, and 9.0 after pre-incubation for 60 min in a Tris–HCl buffer system, respectively. It maintained about 55% residual activity after pre-incubation in an acetate buffer at pH 5.0. CEstKAD01 exhibited moderate thermal stability (Fig. 6b). The enzyme retained more than 80% of its initial activity against *p*NP-B after pre-incubation at 50 °C for 60 min. The relative activity of enzyme CEstKAD01 was 50.14 ± 4.36% after pre-incubation at same temperature for 120 min. The half-life of CEstKAD01 at 60 °C was calculated to be 69.10 min. Results showed that CEstKAD01 is more stable than many other mesophilic esterases identified by functional metagenomics. Jia et al. [56] determined that the remaining activity of Est903 from a paper mill sludge metagenomic library was about 60% after pre-incubation at 50 °C for 60 min. Park et al. [67] observed that est15L from a compost metagenomic library showed less than 10% relative activity after pre-incubation at 40 °C for 10 min. Yao et al. [64] reported that Tan410 esterase lost approximately 46% of its initial activity within 60 min at 60 °C. In another study, Zhang et al. [30] found that EstXT1 from a soil metagenomic library lost more than half of its activity.

The effect of NaCl on the activity of CEstKAD01 was studied in Tris HCl buffer (pH 7.0) at 30 °C (Fig. 7a). The enzyme demonstrated maximum catalytic activity against *p*NP-B in the presence of 6% (~ 1 M) NaCl and maintained 70.77 ± 4.79% of its maximum activity up to 12% (~ 2 M) NaCl. Its relative activity was 27.58 ± 4.52% in the reaction mixture containing 15% (~ 2.5 M) NaCl. The influence

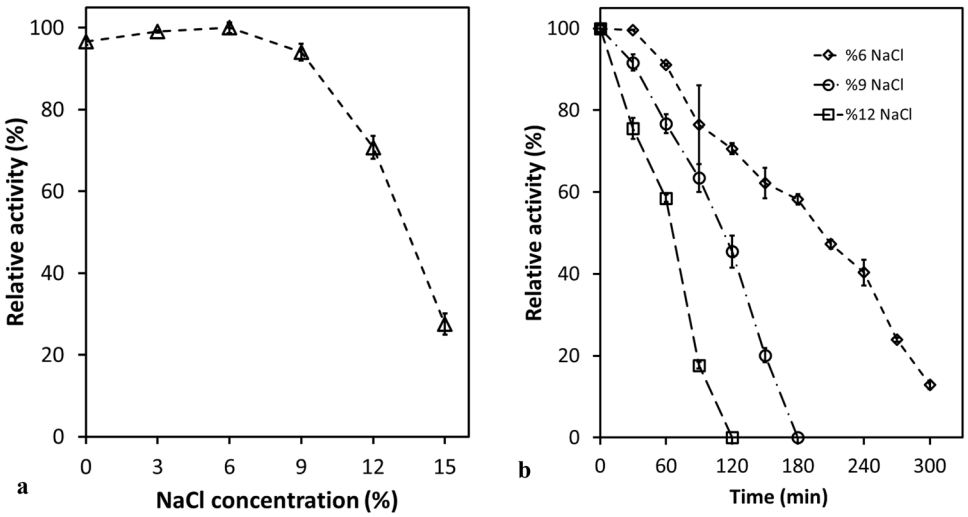

Fig. 7 **a** The influence of NaCl on the activity of CEstKAD01. The highest catalytic activity against *p*NP-B was assumed as 100%. **b** The effect of NaCl on CEstKAD01 stability at concentrations of 6% (open diamonds), 9% (open circles), and 12% (open squares). The initial hydrolytic activity of CEstKAD01 against *p*NP-B was considered 100%. Each value indicates the average of triplicate experiments and the error bars show the standard deviations

of NaCl on the stability of CEstKAD01 was determined by measuring the residual activity after pre-incubation with NaCl at final concentrations of 6, 9, and 12% (w/v) (Fig. 7b). The relative esterase activity of CEstKAD01 was 91.06 ± 0.27% after pre-incubation with 6% NaCl for 60 min. Under the same conditions, it retained more than 50% of its initial activity after pre-incubation for 180 min. CEstKAD01 exhibited 76.74 ± 2.32 and 58.52 ± 0.89% activity after pre-incubation with NaCl at 9 and 12% final concentrations for 60 min, respectively. It was not surprising that CEstKAD01 could remain relatively active and stable in the presence of NaCl since it was associated with bacteria that colonized plastic surfaces in the marine environments [68, 69]. The halotolerant feature of CEstKAD01 may be due to the abundance of negatively charged amino acids (aspartic acids + glutamic acids: 44) in its structure. In addition, the low p*I* value and lysine content (1.9%) of the enzyme may also contribute to its relatively active and stable nature in the presence of NaCl [70].

The effect of metal ions on CEstKAD01 is illustrated in Fig. 8a. Among metal ions, Mg^{2+}, Mn^{2+}, and Ca^{2+} enhanced the activity of CEstKAD01. On the other hand, the enzyme was significantly inhibited by Cu^{2+} and Hg^{2+}. K^{+}, Zn^{2+}, and Li^{2+} had little influence on the enzyme activity.

As depicted in Fig. 8b, the activity of the CEstKAD01 against *p*NP-B was over 80% after the enzyme was pre-incubated with 1 mM of EDTA, DTT, SDS, and Biotin. Like many other esterases or cutinases, CEstKAD01 was strongly inhibited by PMSF, a classical serin hydrolase inactivator.

Analysis performed to evaluate the effect of proteases on CEstKAD01 stability showed that the enzyme lost only 10.12 ± 1.82% of its activity after pre-incubation with 5 U proteinase K at 30 °C for 60 min. The relative activity of the enzyme pre-incubated with 10 and 20 U proteinase K was still over 50%. However, an increase in proteinase K concentration from 20 to 30 U caused a significant decrease (83.87 ± 3.86%) in the activity of CEstKAD01. Results showed that CEstKAD01 could be helpful to for

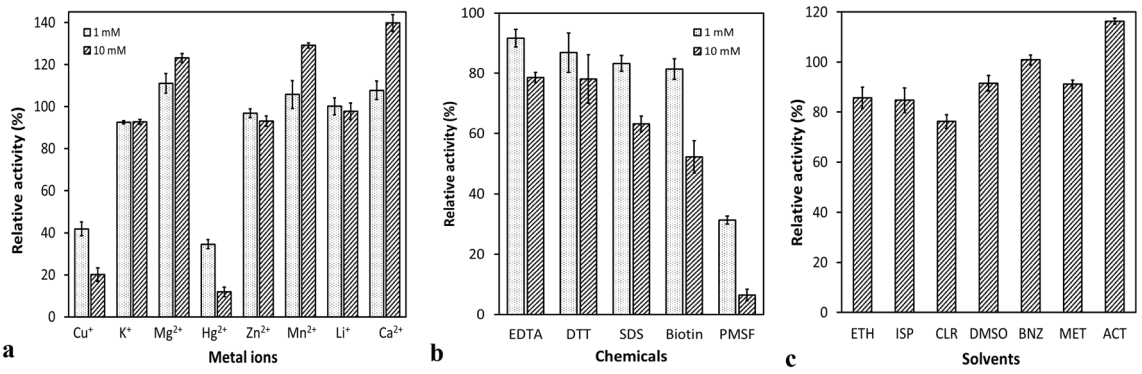

Fig. 8 The effect of metal ions (**a**) and chemicals (**b**) and solvents (**c**) on CEstKAD01 activity. The activity of CEstKAD01 pre-incubated without any additive was considered 100%. Each value indicates the mean value of triplicate experiments and the error bars indicate the standard deviations (*ETH* ethanol, *ISP* isopropanol, *CLR* chloroform, *BNZ* benzene, *MET* methanol, and *ACT* acetone)

environmental biotechnology applications and the detergent industry [41].

The influence of various solvents on CEstKAD01 stability was investigated (Fig. 8c). Benzene showed no significant effect on CEstKAD01. Pre-incubation of CEstKAD01 with ethanol, isopropanol, chloroform, DMSO, and methanol caused a slight decrease (< 25%) in its activity. On the other hand, CEstKAD01 activity increased after pre-incubation with acetone. A similar effect of acetone was reported for Tan410 esterase [63]. Results showed that CEstKAD01 tolerates solvents better than other metagenome-derived esterases [66, 71–73].

The concentration of fatty acids released from 1 g apple cutin was 1.96 ± 0.08, 3.87 ± 0.10, and 5.39 ± 0.18 mM after hydrolysis with 1 mg CEstKAD01 for 60, 90, and 120 min, respectively. Kinetic parameters were investigated by assaying the enzyme activity at varying *p*NP-B concentrations. Results showed that CEstKAD01 exhibited classical Michael-Menten-type kinetics (Supplementary Material 13). Moreover, Michaelis–Menten constant (K_m) and maximum velocity (V_{max}) values of the enzyme were calculated to be 1.48 mM and 20.37 µmol/min, respectively. It is desired that the K_m values of the enzymes to be used in biotechnological applications are between 0.01 and 0.1 mM [74]. The K_m of est3S from a cow rumen metagenomics library was reported to be 2.31 mM [54]. In contrast, km values were about 0.75 mM for E25 [75] and EST5 [76] from metagenomic libraries of sea surface sediment and microbial consortium specialized in diesel oil degradation, respectively.

In summary, its stability in wide pH ranges, salt tolerance, ability to exhibit activity in the presence of many metals, insensitivity to various chemicals, and compatibility with organic solvents make CEstKAD01 valuable for many environmental and industrial applications. It can be used to degrade various organic pollutants, including antibiotics, phthalates, pesticides, and diesel, in saline and alkali environments like salt marshes, coastal regions, and industrial sites with high content. In the food industry, it can assist in the breakdown of plant-based coatings, such as wax or cuticle residues, on fruits and vegetables, thus enhancing the shelf life and appearance of these products. It also can improve the fragrance of dairy products, modifying fatty acids and compounds. It can enhance the efficiency of cleaning products used in hard water. In addition, the enzyme can be integrated into cosmetics to facilitate the layering of fragrances in perfumes, stability of emulsions in lotions, reduce the greasy in sunscreen, relieve sticky in creams, and enhance the absorption of bioactive compounds in anti-aging products.

Plastic Degradability Potential of CEstKAD01

Weight losses in PS, HDPE, LDPE, and PVC pieces by incubation with CEstKAD01 at 30 °C under 120 rpm shaking conditions for 30 days are illustrated in Fig. 9. Percentage weight loss was recorded to be 6.94 ± 0.55, 8.71 ± 0.56, 7.47 ± 0.47, and 9.22 ± 0.18% for PS, HDPE, LDPE, and PVC pieces, respectively. In the majority of previous studies, researchers have focused on the use of microorganisms in the biodegradation of plastics. It has been reported that *Lysinibacillus* sp. JJY0216 [77], *B. amyloliquefaciens* [78], *B. subtilis* ATCC6051 [79], *B. licheniformis* ATCC14580 [79], *Rhodococcus ruber* [80], and *Bacillus cereus* NJD1 [81] reduced the weight of LDPE by approximately 9, 1, 7.5, 3.49, 2.83, and 43%, respectively. Liu et al. [82] have found that *Gordonia* sp. and *Novosphingobium* sp. cause up to a 7.73% decrease in the weight of PS films. In one of the latest studies, Gupta et al. [83] reported that a weight loss of 1.83% was observed in the HDPE film incubated with *Bacillus cereus* CGK5 for 90 days. In another study, Nyamjav et al. [84] determined that the weight loss of the PVC sheets was 2.06%, incubated with *Citrobacter koseri* isolated from *Zophobas atratus* larvae. However, there are few studies on the degradation of plastics with pure enzymes in the literature [85]. Our results show that enzymatic treatment can be an alternative to using microorganisms for PS, HDPE, LDPE, and PVC biodegradation.

The surfaces of plastic pieces were visualized by FESEM after incubation in buffer with (treated) and without (untreated) CEstKAD01 at 30 °C under 120 rpm shaking conditions for 30 days. As seen in Fig. 10a–h, the surfaces of untreated PS, HDPE, LDPE, and PVC pieces were smooth. On the other hand, FESEM micrographs of plastics treated

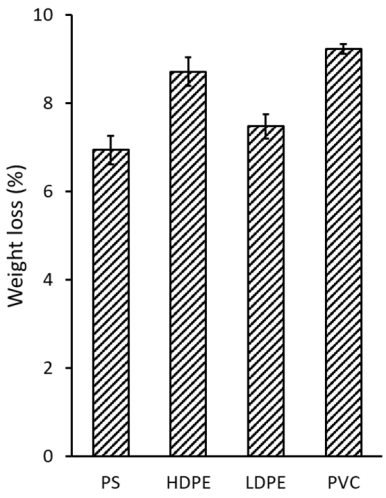

Fig. 9 Weight loss of PS, HDPE, LDPE, and PVC pieces by incubation with CEstKAD01 in 50 mM phosphate buffer (pH 7.0) at 30 °C under 120 rpm shaking conditions for 30 days

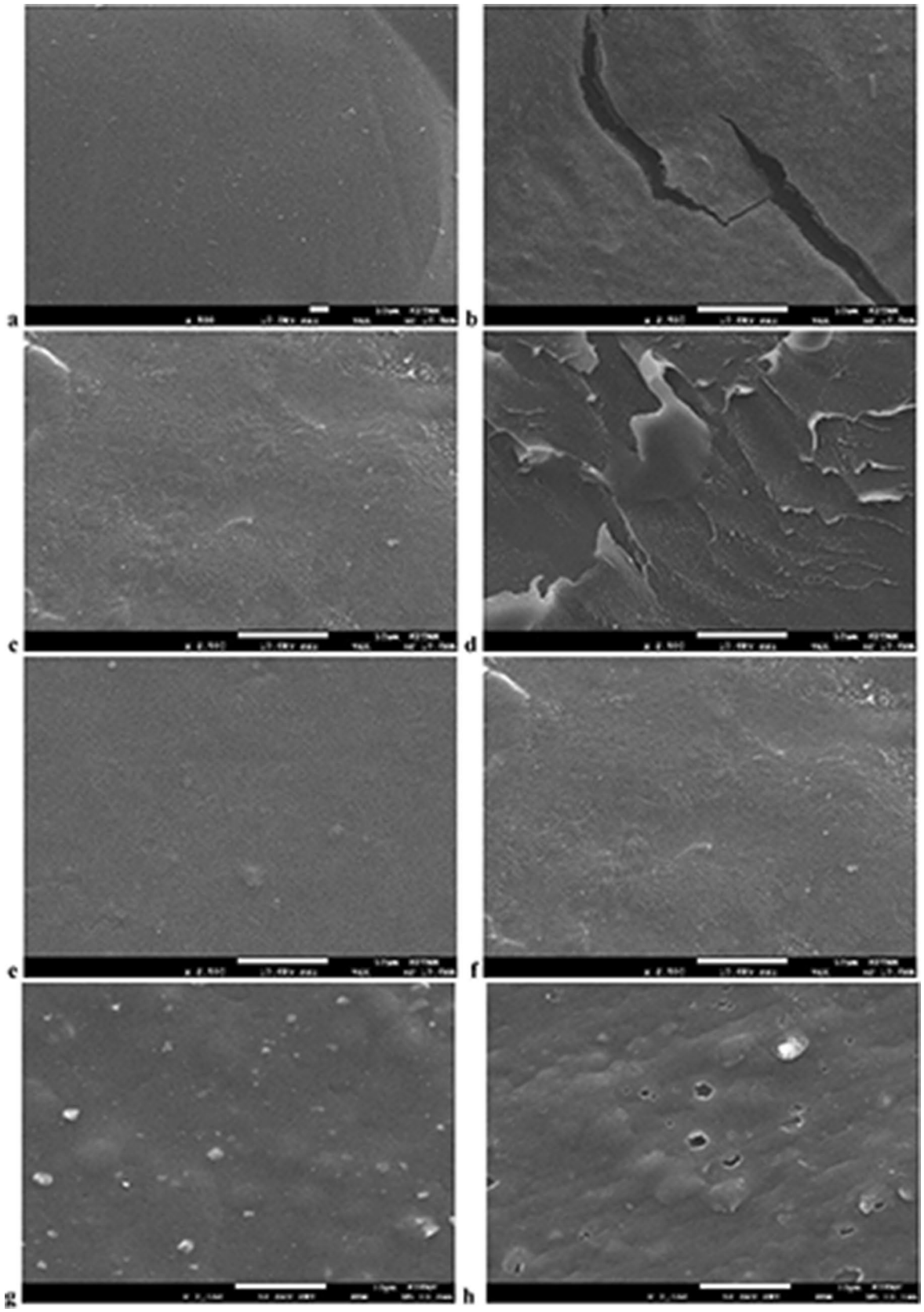
a
b
c
d
e
f
g
h

◂**Fig. 10** Scanning electron micrographs of plastics incubated in 50 mM phosphate buffer (pH 7.0) containing CEstKAD01 (1 U/mL) at 30 °C for 30 days (treated). Pieces incubated in enzyme-free buffer under the same condition were used as control (untreated). Each sample is displayed in ×2500 magnification. **a** Untreated PS, **b** treated PS, **c** untreated HDPE, **d** treated HDPE, **e** untreated LDPE, **f** treated LDPH, **g** untreated PVC, **h** treated PVC

with CEstKAD01 exhibited roughness. In addition to surface erosion, it was observed that enzymatic treatment caused the formation of some holes and pits on the plastic surfaces.

FTIR spectrums of PS control (PS-C) and PS treated with the enzyme (PS-E) are shown in Fig. 11a. Peaks of PS-C at 3082, 3060, and 3025 cm^{-1}, which correspond to aromatic C–H stretches, shifted to 3085, 3062, and 3026 cm^{-1} after enzymatic treatment. A peak observed at 2921 cm^{-1}, characteristic of CH_2 asymmetric C–H stretch, in the spectrum of PS-C was seen at 2923 cm^{-1} in the spectrum of PS-E. The weak peak at 2850 cm^{-1} in the PS-C spectrum disappeared with the enzymatic treatment. A shift in the peaks at 1493 and 1452 cm^{-1}, associated with stretching vibration of C=C and C–H of the aromatic ring, and a decrease in their intensities were observed. In the spectrum of PS-E, the intensity of peaks at 755 and 696, corresponding to aromatic out-of-plane C–H bend and aromatic ring bend, was lower than that of in the spectrum of PS-C. Furthermore, an additional peak associated with the carbonyl group (C=O) appeared in the spectrum after enzymatic treatment.

FTIR spectrums of HDPE control (HDPE-C) and HDPE treated with the enzyme (HDPE-E) are compared in Fig. 11b. A sharp peak at 2914 cm^{-1} and 1057, which arose from the stretching vibration of C–H and C–O, shifted to 2917 and 1066 after enzymatic treatment. The point of the peak at 2850 cm^{-1}, attributed to the stretching vibration of C–H, in the spectrum of HDPE-C, did not change, but its intensity decreased slightly in the spectrum of HDPE-E. Enzymatic treatment caused the formation of a new peak at 1150 cm^{-1}, responsible for C–O stretching, and the broadening of a peak at 1394 corresponding to O–H bending. Similar phenomena and changes were observed for LDPE control (LDPE-C) and LDPE treated with the enzyme (LDPE-E) (Fig. 11c). In addition, a shift in the peaks at 1460 cm^{-1}, corresponds to C–H scissoring, and a slight decrease in its intensity were monitored in the FTIR spectrum of LDPE-E, as distinct from LDPE-C.

As shown in Fig. 11d, it is seen that enzymatic treatment causes various alterations in the FTIR spectrum of PVC. Among the prominent peaks, those at 3676 (O–H stretching), 2916 (C–H stretching) and 2271 (S–C≡N stretching) and 1451 cm^{-1} (C–H bending), and 874 (C=C bending) cm^{-1} displayed a significant shift after enzymatic treatment. A substantial decrease in the intensity of the peaks located at 2950 (C–H stretching), 1380 (C–H bending), 1050 (CO–O–CO stretching), and 874 cm^{-1} in the FTIR spectrum of PVC-C was observed with enzymatic treatment. On the other hand, it was determined that enzymatic treatment slightly increased the intensity of the peaks at 2271, 973 (C=C bending), 841 (C=C bending), and 809 (C–H bending) cm^{-1}. In addition, new peaks appeared at 3278 (C–H stretching), 2801 (N–H stretching), and 1536 (N–O stretching) cm^{-1} in the FTIR spectrum of PVC-C, unlike that of PVC-C.

In summary, FTIR analysis showed that CEstKAD01, a cutinolytic carboxyl esterase derived from microplastic-associated metagenome, is capable of degrading PS, HDPE, LDPE, and PVC. Moreover, the large and broad peaks at 300–3500 cm^{-1} in the FTIR analyses of the plastic pieces after enzymatic treatment indicate that the plastic pieces' hydrophilicity increased due to enzymatic degradation.

Previously, several types of plastics-degrading enzymes have been reported. Schmidt et al. [86] reported that LC cutinase caused weight losses of up to 4.9% of polyurethane (PU) within a reaction time of 200 h at 70 °C. Furukawa et al. [87] found that TfCut2 resulted in 7.5% weight loss of lcPET film after a 24-h reaction. Blázquez-Sánchez et al. [88] reported that an enzyme (11 µg/mL) from *Moraxella* sp. TA144 caused weight loss of PET film (~45 mg) after incubation in 1 M potassium phosphate buffer for 24 h. It has been reported that PHL7, an enzyme identified from the compost metagenome, completely degrades PET in 18 h [89]. In another study, Zhang et al. [90] detected that the metagenome-derived esterase PET40 released 50.41 ± 10.21 µm of TPA, which are monomeric degradation products, from PET in a 72-h at 40 °C. As can be seen from the examples, all these enzymes act on plastics with heterochain backbones (C–X). In contrast, CEstKAD01 acts on plastics with homochain backbones (C–C), which are more difficult to degrade than plastics with heterochain backbones due to their high crystallinity. Moreover, it has a higher potential for use in environmental applications than its peers mentioned above, as plastics with homochain backbones are consumed more than other plastics on a global scale [91].

In high temperatures (50–70 °C), the enzyme accesses the polymer chain more efficiently due to the increasing viscosity of plastic [89]. Therefore, many researchers have focused on identifying thermo-tolerant plastic-degrading enzymes. However, plastic-degrading enzymes active at low temperatures, such as CEstKAD01, also have benefits. They could offer a more economical and eco-friendly solution because they would allow plastics to be recycled slowly at lower temperatures.

Genotoxicity of degradation products

Overall, it is desired that the products released from the substrate due to enzymatic activity are not toxic or genotoxic to

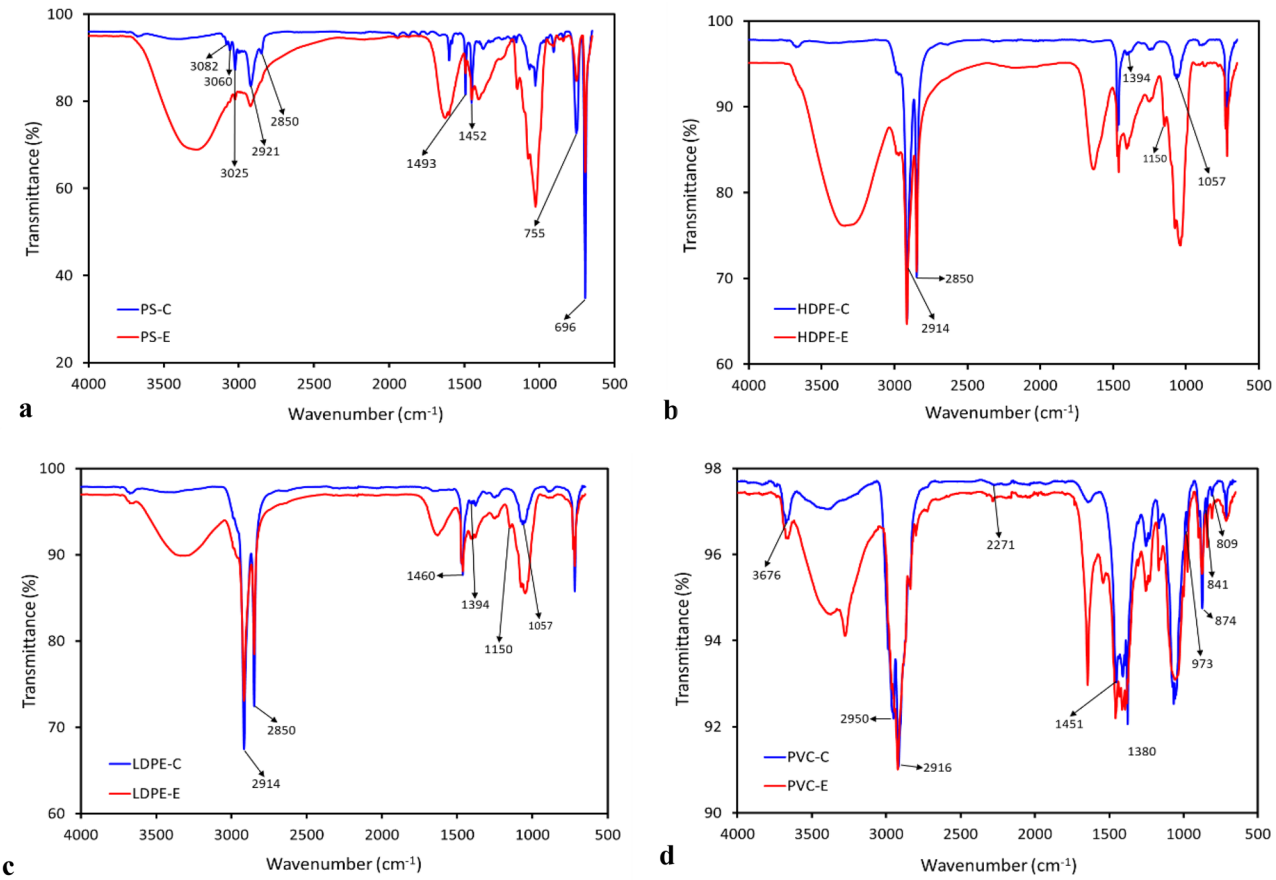

Fig. 11 FTIR analysis of plastic pieces incubated in 50 mM phosphate buffer (pH 7.0) containing CEstKAD01 (1 U/mL) at 30 °C for 30 days (treated). Plastic pieces incubated without CEstKAD01 under the same conditions were used to be control (untreated). **a** Untreated PS (PS-C) and treated PS (PS-E), **b** untreated HDPE (HDPE-C) and treated HDPE (HDPE-E), **c** untreated LDPE (LDPE-C) and treated LDPH (LDPE-E), **d** untreated PVC (PVC-C) and treated PVC (PVC-E)

living things in the application of enzymes for the remediation. Genotoxicity of degradation products was evaluated by comparison of DNA damage in *S. cerevisiae* cells. The DNA damage was measured as the mean tail length of comet-like nuclei in lysed cells. One hundred nuclei were counted for each experimental set under fluorescence microscopy (Olympus BX40, Hamburg, Germany). No significant difference was detected in DNA damage in cells exposed to degradation products or not (negative control). In addition, it was measured that the tailing in the nuclei of these cells was considerably less (Data was not shown). However, a significant increase in DNA damage was observed when yeast cells were exposed to H_2O_2 (positive control). Results showed that degradation products were not genotoxic to *S. cerevisiae* cells. Representative fluorescent microscopy images used to detect DNA damage in cells are shown in Fig. 12a–f.

While many studies exist about the biodegradation of plastics in the literature, few toxicological reports of degradation products exist. In a study, Shahnawaz et al. [92] reported no significant change in the percent germination rate of sorghum seeds exposed to PE degradation products. Khandare et al. [93] reported that the germination of *Vigna radiata* seeds was not significantly affected by degradation products of PVC (PVCDP), but the germination index and elongation inhibition rate decreased in seeds exposed to PVCDP. They also found that the growth rate and chlorophyll content of *Ulva lactuca* after exposure to PVCDP increased. On the other hand, Peng et al. [94] reported that PVCDP could exhibit a bactericidal effect against some gut bacteria in *Tenebrio molitor* larvae.

Conclusion

The presented functional metagenomics-based study led to the discovery of a new cutinolytic esterase CEstKAD01. After statistical optimization, the enzyme was successfully overexpressed in *E. coli* BL21 (DE3). CEstKAD01 was highly active over a wide temperature and pH range. The enzyme displayed outstanding tolerance against

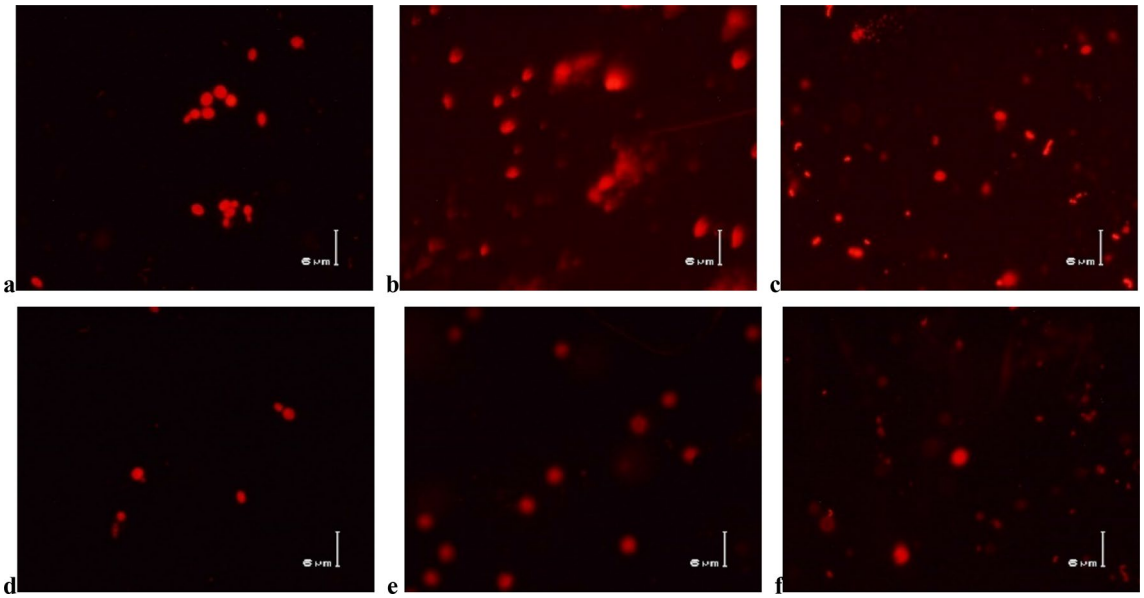

Fig. 12 Representative fluorescent microscopy images of nuclei to detect DNA damage in *S. cerevisiae* cells after experiments. Images of nuclei from cells in negative (**a**) and positive controls (**b**) and exposed to degradation products of PS (**c**), HDPE (**d**), LDPE (**e**), and PVC (**f**)

NaCl, metal ions, inhibitory chemicals, and solvents. These properties of the enzyme make it versatile biocatalysts for many applications in textile, food, beverage, biofuel, cosmetic, pharmaceutical, chemical, and detergent industries. CEstKAD01 showed PS, HDPE, LDPE, and PVC degradation capacity. Degradation products did not show genotoxic effects. Within this framework, the catalytic mechanism of CEstKAD01 could be elucidated by structural analyses and mutagenesis. The enzyme could be converted to broad-range biocatalysts for plastic recycling through computational redesign. It may help design enzyme–polymer hybrid materials with ad-hoc formulations prone to facilitate degradation. Moreover, with further optimization and scale-up studies, CEstKAD01 could be made suitable for real-world applications.

Supplementary Information The online version contains supplementary material available at https://doi.org/10.1007/s12033-023-00916-7.

Author Contributions Conceptualization: AOA; Methodology: AOA, SK-A, TD; Formal analysis and investigation: AOA, SK-A, and FŞ; Writing—original draft preparation: AOA and SK-A; Writing—review and editing: MT, TD, AEK, AK; Funding acquisition and resources: AOA; Supervision: AEK, AK, MT.

Funding This study was supported by the Scientific and Technological Research Council of Türkiye (TUBİTAK) under Project No. 120Z329.

Data Availability Data will be available by made on request.

Declarations

Conflict of Interest The authors declare that no competing interests in the present research article.

Ethical Approval The presented article does not contain any studies involving animal or human participants performed by any of the authors.

Consent for Participation Not applicable.

Consent for Publication Not applicable.

References

1. Chigwada, A. D., & Tekere, M. (2023). The plastic and microplastic waste menace and bacterial biodegradation for sustainable environmental clean-up a review. *Environmental Research, 231*, 116110.
2. Kumar, M., Bolan, S., Padhye, L. P., Konarova, M., Foong, S. Y., Lam, S. S., Wagland, S., Cao, R., Li, Y., Batalha, N., Ahmed, M., Pandey, A., Siddique, K. H. M., Wang, H., Rinklebe, J., & Bolan, N. (2023). Retrieving back plastic wastes for conversion to value added petrochemicals: Opportunities, challenges and outlooks. *Applied Energy, 345*, 121307.
3. Cole, M., Lindeque, P., Halsband, C., & Galloway, T. S. (2011). Microplastics as contaminants in the marine environment: A review. *Marine Pollution Bulletin, 62*(12), 2588–2597.
4. Iyer, H., Grandgeorge, P., Jimenez, A. M., Campbell, I. R., Parker, M., Holden, M., Venkatesh, M., Nelsen, M., Nguyen, B., & Roumeli, E. (2023). Fabricating strong and stiff bioplastics from whole spirulina cells. *Advanced Functional Materials*, 2302067.
5. Tejaswini, M. S. S. R., Pathak, P., Ramkrishna, S., & Ganesh, P. S. (2022). A comprehensive review on integrative approach for sustainable management of plastic waste and its associated externalities. *Science of the Total Environment, 825*, 153973.
6. Borrelle, S. B., Ringma, J., Law, K. L., Monnahan, C. C., Lebreton, L., McGivern, A., Murphy, E., Jambeck, J., Leonard, G. H., Hilleary, M. A., Eriksen, M., Possingham, H. P., Frond, H. D., Gerber, L. R., Polidoro, B., Tahir, A., Bernard, M., Mallos, N., Barnes, M., & Rochman, C. M. (2020). Predicted growth in

plastic waste exceeds efforts to mitigate plastic pollution. *Science, 369*(6510), 1515–1518.
7. Kibria, M. G., Masuk, N. I., Safayet, R., Nguyen, H. Q., & Mourshed, M. (2023). Plastic waste: Challenges and opportunities to mitigate pollution and effective management. *Int. J. Environ. Res., 17*(1), 20.
8. Rosenboom, J. G., Langer, R., & Traverso, G. (2022). Bioplastics for a circular economy. *Nature Reviews Materials, 7*(2), 117–137.
9. Pan, D., Su, F., Liu, C., & Guo, Z. (2020). Research progress for plastic waste management and manufacture of value-added products. *Advanced Composites and Hybrid Materials, 3*, 443–461.
10. Zhang, Y., Pedersen, J. N., Eser, B. E., & Guo, Z. (2022). Biodegradation of polyethylene and polystyrene: From microbial deterioration to enzyme discovery. *Biotechnology Advances, 60*, 107991.
11. Evode, N., Qamar, S. A., Bilal, M., Barceló, D., & Iqbal, H. M. (2021). Plastic waste and its management strategies for environmental sustainability. *Case Studies in Chemical and Environmental Engineering, 4*, 100142.
12. Plastics Europa. (2022). Plastics-the Facts. https://plasticseurope.org/knowledge-hub/plastics-the-facts-2022/
13. Yang, J., Yang, Y., Wu, W. M., Zhao, J., & Jiang, L. (2014). Evidence of polyethylene biodegradation by bacterial strains from the guts of plastic-eating waxworms. *Environmental Science and Technology, 48*(23), 13776–13784.
14. Zhang, H., Perez-Garcia, P., Dierkes, R. F., Applegate, V., Schumacher, J., Chibani, C. M., Sternagel, S., Preuss, L., Weigert, S., Vollstedt, C., Almeida, A., Höcker, B., Hallam, S. J., Schmitz-Streit, R. A., Smits, S. H. J., Chow, J., & Streit, W. R. (2022). The Bacteroidetes *Aequorivita* sp. and *Kaistella jeonii* produce promiscuous esterases with PET-hydrolyzing activity. *Frontiers in Microbiology, 12*, 803896.
15. Cheng, Y., Chen, J., Bao, M., & Li, Y. (2022). Surface modification ability of *Paracoccus* sp. indicating its potential for polyethylene terephthalate degradation. *International Biodeterioration and Biodegradation, 173*, 105454.
16. Oluwole, O. A., Oluyege, J. O., & Olowomofe, T. O. (2022). Biodegradation of polyethylene based films used in water packaging by dumpsite bacteria. *Bioremediation Journal*, 1–13.
17. Saeed, S., Iqbal, A., & Deeba, F. (2022). Biodegradation study of polyethylene and PVC using naturally occurring plastic degrading microbes. *Archives of Microbiology, 204*(8), 497.
18. Wróbel, M., Szymańska, S., Kowalkowski, T., & Hrynkiewicz, K. (2023). Selection of microorganisms capable of polyethylene (PE) and polypropylene (PP) degradation. *Microbiological Research, 267*, 127251.
19. Wang, P., Liu, J., Han, S., Wang, Y., Duan, Y., Liu, T., Hou, L., Zhang, Z., Li, L., & Lin, Y. (2023). Polyethylene mulching film degrading bacteria within the plastisphere: Co-culture of plastic degrading strains screened by bacterial community succession. *Journal of Hazardous Materials, 442*, 130045.
20. Ahmad, A., Tsutsui, A., Iijima, S., Suzuki, T., Shah, A. A., & Nakajima-Kambe, T. (2019). Gene structure and comparative study of two different plastic-degrading esterases from *Roseateles depolymerans* strain TB-87. *Polymer Degradation and Stability, 164*, 109–117.
21. Adıgüzel, A. O., & Tunçer, M. (2017). Purification and characterization of cutinase from *Bacillus* sp. KY0701 isolated from plastic wastes. *Preparative Biochemistry and Biotechnology, 47*(9), 925–933.
22. Adıgüzel, A. O. (2020). Production and characterization of thermo-, halo-and solvent-stable esterase from *Bacillus mojavensis* TH309. *Biocatalysis and Biotransformation, 38*(3), 210–226.
23. Carr, C. M., de Oliveira, B. F. R., Jackson, S. A., Laport, M. S., Clarke, D. J., & Dobson, A. D. (2022). Identification of BgP, a cutinase-like polyesterase from a deep-sea sponge-derived actinobacterium. *Frontiers in Microbiology, 13*, 1194.
24. Ufarté, L., Laville, É., Duquesne, S., & Potocki-Veronese, G. (2015). Metagenomics for the discovery of pollutant degrading enzymes. *Biotechnology Advances, 33*(8), 1845–1854.
25. Richter, P. K., Blázquez-Sánchez, P., Zhao, Z., Engelberger, F., Wiebeler, C., Künze, G., Frank, R., Krinke, D., Frezzotti, E., Lihanova, Y., Falkenstein, P., Matysik, J., Zimmermann, W., Sträter, N., & Sonnendecker, C. (2023). Structure and function of the metagenomic plastic-degrading polyester hydrolase PHL7 bound to its product. *Nature Communications, 14*(1), 1905.
26. Wani, A. K., Akhtar, N., Naqash, N., Rahayu, F., Djajadi, D., Chopra, C., Singh, R., Mulla, S. I., Sher, F., & Américo-Pinheiro, J. H. P. (2023). Discovering untapped microbial communities through metagenomics for microplastic remediation: Recent advances, challenges, and way forward. *Environmental Science and Pollution Research*, 1–24.
27. Delacuvellerie, A., Geron, A., Gobert, S., & Wattiez, R. (2022). New insights into the functioning and structure of the PE and PP plastispheres from the Mediterranean Sea. *Environmental Pollution, 295*, 118678.
28. Zhang, C., Mu, Y., Li, T., Jin, F. J., Jin, C. Z., Oh, H. M., Lee, H. G., & Jin, L. (2023). Assembly strategies for polyethylene-degrading microbial consortia based on the combination of omics tools and the "Plastisphere." *Frontiers in Microbiology, 14*, 1181967.
29. Rüthi, J., Rast, B. M., Qi, W., Perez-Mon, C., Pardi-Comensoli, L., Brunner, I., & Frey, B. (2023). The plastisphere microbiome in alpine soils alters the microbial genetic potential for plastic degradation and biogeochemical cycling. *Journal of Hazardous Materials, 441*, 129941.
30. Zhang, Y., Ding, L., Yan, Z., Zhou, D., Jiang, J., Qiu, J., & Xin, Z. (2023). Identification and characterization of a novel carboxylesterase belonging to family VIII with promiscuous acyltransferase activity toward cyanidin-3-o-glucoside from a soil metagenomic library. *Applied Biochemistry and Biotechnology, 195*(4), 2432–2450.
31. Debeljak, P., Pinto, M., Proietti, M., Reisser, J., Ferrari, F. F., Abbas, B., van Loosdrecht, M. C. M., Slat, B., & Herndl, G. J. (2017). Extracting DNA from ocean microplastics: A method comparison study. *Analytical Methods, 9*(9), 1521–1526.
32. Hancock, J. M., & Bishop, M. J. (2004). *HMMer. Dictionary of bioinformatics and computational biology*. Wiley.
33. Paysan-Lafosse, T., Blum, M., Chuguransky, S., Grego, T., Pinto, B. L., Salazar, G. A., Bileschi, M. L., Bork, P., Bridge, A., Colwell, L., Gough, J., Haft, D. H., Letunić, I., Marchler-Bauer, A., Mi, H., Natale, D. A., Orengo, C. A., Pandurangan, A. P., Rivoire, C., … Bateman, A. (2023). InterPro in 2022. *Nucleic Acids Research, 51*(D1), D418–D427.
34. Altschul, S. F., Gish, W., Mille, W., Myers, E. W., & Lipman, D. J. (1990). Basic local alignment search tool. *Journal of Molecular Biology, 3*, 403–410.
35. Waterhouse, A. M., Procter, J. B., Martin, D. M., Clamp, M., & Barton, G. J. (2009). *Bioinformatics, 25*(9), 1189–1191.
36. Kumar, S., Stecher, G., Li, M., Knyaz, C., & Tamura, K. (2018). MEGA X: Molecular evolutionary genetics analysis across computing platforms. *Molecular Biology and Evolution, 35*(6), 1547.
37. Noby, N., Hussein, A., Saeed, H., & Embaby, A. M. (2020). Recombinant cold-adapted halotolerant, organic solvent-stable esterase (estHIJ) from *Bacillus halodurans*. *Analytical Biochemistry, 591*, 113554.
38. Kelley, L. A., Mezulis, S., Yates, C. M., Wass, M. N., & Sternberg, M. J. (2015). The Phyre2 web portal for protein modeling, prediction and analysis. *Nature Protocols, 10*(6), 845–858.
39. Waterhouse, A., Bertoni, M., Bienert, S., Studer, G., Tauriello, G., Gumienny, R., Heer, F. T., de Beer, T. A. P., Rempfer, C., Bordoli, R., Lepore, R., & Schwede, T. (2018). SWISS-MODEL: Homology modelling of protein structures and complexes. *Nucleic Acids Research, 46*(W1), W296–W303.

40. Adigüzel, A. O., Könen-Adigüzel, S., Cilmeli, S., Mazmancı, B., Yabalak, E., Üstün-Odabaşı, S., Kaya, N. G., & Mazmancı, M. A. (2023). Heterologous expression, purification, and characterization of thermo-and alkali-tolerant laccase-like multicopper oxidase from *Bacillus mojavensis* TH309 and determination of its antibiotic removal potential. *Archives of Microbiology, 205*(8), 287.
41. Bradford, M. M. (1976). A rapid and sensitive method for the quantitation of microgram quantities of protein utilizing the principle of protein-dye binding. *Analytical Biochemistry, 72*, 248–254.
42. Adıgüzel, A. O., & Tunçer, M. (2017). Production, purification, characterization and usage of a detergent additive of endoglucanase from isolated halotolerant *Amycolatopsis cihanbeyliensis* mutated strain Mut43. *Biocatalysis and Biotransformation, 35*(3), 197–204.
43. Chaudhari, S. A., & Singhal, R. S. (2015). Cutin from watermelon peels: A novel inducer for cutinase production and its physicochemical characterization. *International Journal of Biological Macromolecules, 79*, 398–404.
44. Ribitsch, D., Acero, E. H., Greimel, K., Eiteljoerg, I., Trotscha, E., Freddi, G., Schwab, H., & Guebitz, G. M. (2012). Characterization of a new cutinase from *Thermobifida alba* for PET-surface hydrolysis. *Biocatalysis and Biotransformation., 30*(1), 2–9.
45. Adiguzel, A. O., Adiguzel, S. K., Mazmanci, B., Tunçer, M., & Mazmanci, M. A. (2018). Silver nanoparticle biosynthesis from newly isolated *Streptomyces* genus from soil. *Materials Research Express, 5*(4), 045402.
46. Sulaiman, S., Yamato, S., Kanaya, E., Kim, J. J., Koga, Y., Takano, K., & Kanaya, S. (2012). Isolation of a novel cutinase homolog with polyethylene terephthalate-degrading activity from leaf-branch compost by using a metagenomic approach. *Applied and Environment Microbiology, 78*(5), 1556–1562.
47. Qiu, J., Yang, H., Yan, Z., Shi, Y., Zou, D., Ding, L., Shao, Y., Li, L., Khan, U., Sun, S., & Xin, Z. (2020). Characterization of XtjR8: A novel esterase with phthalate-hydrolyzing activity from a metagenomic library of lotus pond sludge. *International Journal of Biological Macromolecules, 164*, 1510–1518.
48. Park, J. M., Won, S. M., Kang, C. H., Park, S., & Yoon, J. H. (2020). Characterization of a novel carboxylesterase belonging to family VIII hydrolyzing β-lactam antibiotics from a compost metagenomic library. *International Journal of Biological Macromolecules, 164*, 4650–4661.
49. Yan, Z., Ding, L., Zou, D., Qiu, J., Shao, Y., Sun, S., Li, L., & Xin, Z. (2021). Characterization of a novel carboxylesterase with catalytic activity toward di (2-ethylhexyl) phthalate from a soil metagenomic library. *Science of the Total Environment, 785*, 147260.
50. Duan, X., Jiang, Z., Liu, Y., Yan, Q., Xiang, M., & Yang, S. (2019). High-level expression of codon-optimized *Thielavia terrestris* cutinase suitable for ester biosynthesis and biodegradation. *International Journal of Biological Macromolecules, 135*, 768–775.
51. Tan, Y., Henehan, G. T., Kinsella, G. K., & Ryan, B. J. (2021). An extracellular lipase from *Amycolatopsis mediterannei* is a cutinase with plastic degrading activity. *Computational and Structural Biotechnology Journal, 19*, 869–879.
52. Nazarian, Z., & Arab, S. S. (2022). Discovery of carboxylesterases via metagenomics: Putative enzymes that contribute to chemical kinetic resolution. *Process Biochemistry, 121*, 439–454.
53. Liang, X., & Zou, H. (2022). Biotechnological application of cutinase: A powerful tool in synthetic biology. *SynBio, 1*(1), 54–64.
54. Lu, M., Dukunde, A., & Daniel, R. (2019). Biochemical profiles of two thermostable and organic solvent–tolerant esterases derived from a compost metagenome. *Applied Microbiology and Biotechnology, 103*, 3421–3437.
55. Lee, H. Y., Cho, D. Y., Ahmad, I., Patel, H. M., Kim, M. J., Jung, J. G., Jeong, E. H., Haque, M. A., & Cho, K. M. (2021). Mining of a novel esterase (est3S) gene from a cow rumen metagenomic library with organosphosphorus insecticides degrading capability: Catalytic insights by site directed mutations, docking, and molecular dynamic simulations. *International Journal of Biological Macromolecules, 190*, 441–455.
56. Jia, M. L., Zhong, X. L., Lin, Z. W., Dong, B. X., & Li, G. (2019). Expression and characterization of an esterase belonging to a new family via isolation from a metagenomic library of paper mill sludge. *International Journal of Biological Macromolecules, 126*, 1192–1200.
57. Chen, C., Yu, G., Guo, Z., Yang, Q., Su, W., Xie, Q., Yang, G., Ren, Y., & Li, H. (2022). Expression, characterization, fermentation, immobilization, and application of a novel esterase Est804 from metagenomic library in pesticide degradation. *Frontiers in Microbiology, 13*, 922506.
58. Distaso, M., Cea-Rama, I., Coscolín, C., Chernikova, T. N., Tran, H., Ferrer, M., Sanz-Aparicio, J., & Golyshin, P. N. (2023). The mobility of the cap domain is essential for the substrate promiscuity of a family IV esterase from sorghum rhizosphere microbiome. *Applied and Environmental Microbiology, 89*, e0180722.
59. Yu, E. Y., Kwon, M. A., Lee, M., Oh, J. Y., Choi, J. E., Lee, J. Y., Song, B. K., Hahm, D. H., & Song, J. K. (2011). Isolation and characterization of cold-active family VIII esterases from an arctic soil metagenome. *Applied Microbiology and Biotechnology, 90*, 573–581.
60. Privé, F., Newbold, C. J., Kaderbhai, N. N., Girdwood, S. G., Golyshina, O. V., Golyshin, P. N., Scollan, N. D., & Huws, S. A. (2015). Isolation and characterization of novel lipases/esterases from a bovine rumen metagenome. *Applied Microbiology and Biotechnology, 99*, 5475–5485.
61. Pereira, M. R., Maester, T. C., Mercaldi, G. F., de Macedo Lemos, E. G., Hyvönen, M., & Balan, A. (2017). From a metagenomic source to a high-resolution structure of a novel alkaline esterase. *Applied Microbiology and Biotechnology, 101*, 4935–4949.
62. Tutuncu, H. E., Balci, N., Tuter, M., & Karaguler, N. G. (2019). Recombinant production and characterization of a novel esterase from a hypersaline lake, Acıgöl, by metagenomic approach. *Extremophiles, 23*, 507–520.
63. Kryukova, M. V., Petrovskaya, L. E., Kryukova, E. A., Lomakina, G. Y., Yakimov, S. A., Maksimov, E. G., Boyko, K. M., Popov, V. O., Dolgikh, D. A., & Kirpichnikov, M. P. (2019). Thermal inactivation of a cold-active esterase PMGL3 isolated from the permafrost metagenomic library. *Biomolecules, 9*(12), 880.
64. Yao, J., Gui, L., & Yin, S. (2021). A novel esterase from a soil metagenomic library displaying a broad substrate range. *AMB Express, 11*(1), 1–10.
65. De Santi, C., Ambrosino, L., Tedesco, P., de Pascale, D., Zhai, L., Zhou, C., Xue, Y., & Ma, Y. (2015). Identification and characterization of a novel salt-tolerant esterase from a Tibetan glacier metagenomic library. *Biotechnology Progress, 31*(4), 890–899.
66. Liaw, R. B., Chen, J. C., & Cheng, M. P. (2022). Molecular cloning and characterization of a new family VI esterase from an activated sludge metagenome. *Microorganisms, 10*(12), 2403.
67. Park, J. E., Jeong, G. S., Lee, H. W., & Kim, H. (2021). Biochemical characterization of a family IV esterase with R-form enantioselectivity from a compost metagenomic library. *Applied Biological Chemistry, 64*, 1–16.
68. Okamura, Y., Kimura, T., Yokouchi, H., Meneses-Osorio, M., Katoh, M., Matsunaga, T., & Takeyama, H. (2010). Isolation and characterization of a GDSL esterase from the metagenome of a marine sponge-associated bacteria. *Marine Biotechnology, 12*, 395–402.
69. De Santi, C., Altermark, B., Pierechod, M. M., Ambrosino, L., de Pascale, D., & Willassen, N. P. (2016). Characterization of

a cold-active and salt tolerant esterase identified by functional screening of Arctic metagenomic libraries. *BMC Biochemistry, 17*, 1–13.
70. Lu, M., & Daniel, R. (2021). A novel carboxylesterase derived from a compost metagenome exhibiting high stability and activity towards high salinity. *Genes, 12*(1), 122.
71. Ouyang, L. M., Liu, J. Y., Qiao, M., & Xu, J. H. (2013). Isolation and biochemical characterization of two novel metagenome-derived esterases. *Applied Biochemistry and Biotechnology, 169*, 15–28.
72. Sarkar, J., Dutta, A., Pal Chowdhury, P., Chakraborty, J., & Dutta, T. K. (2020). Characterization of a novel family VIII esterase EstM2 from soil metagenome capable of hydrolyzing estrogenic phthalates. *Microbial Cell Factories, 19*, 1–12.
73. Boyko, K. M., Kryukova, M. V., Petrovskaya, L. E., Kryukova, E. A., Nikolaeva, A. Y., Korzhenevsky, D. A., Lomakina, G. Y., Novototskaya-Vlasova, K., Rivkina, E., Dolgikh, D., Kirpichnikov, M. P., & Popov, V. O. (2021). Structural and biochemical characterization of a cold-active PMGL3 esterase with unusual oligomeric structure. *Biomolecules, 11*(1), 57.
74. Asoodeh, A., & Ghanbari, T. (2013). Characterization of an extracellular thermophilic alkaline esterase produced by *Bacillus subtilis* DR8806. *Journal of Molecular Catalysis B Enzymatic, 85*, 49–55.
75. Li, P. Y., Ji, P., Li, C. Y., Zhang, Y., Wang, G. L., Zhang, X. Y., Xie, B. B., Qin, Q. L., Chen, X. L., Zhou, B. C., & Zhang, Y. Z. (2014). Structural basis for dimerization and catalysis of a novel esterase from the GTSAG motif subfamily of the bacterial hormone-sensitive lipase family. *Journal of Biological Chemistry, 289*(27), 19031–19041.
76. Maester, T. C., Pereira, M. R., Malaman, A. M. G., Borges, J. P., Pereira, P. A. M., & Lemos, E. G. (2020). Exploring metagenomic enzymes: A novel esterase useful for short-chain ester synthesis. *Catalysts, 10*(10), 1100.
77. Jeon, J. M., Park, S. J., Choi, T. R., Park, J. H., Yang, Y. H., & Yoon, J. J. (2021). Biodegradation of polyethylene and polypropylene by *Lysinibacillus* species JJY0216 isolated from soil grove. *Polymer Degradation and Stability, 191*, 109662.
78. Nowak, B., Pająk, J., Drozd-Bratkowicz, M., & Rymarz, G. (2011). Microorganisms participating in the biodegradation of modified polyethylene films in different soils under laboratory conditions. *International Biodeterioration and Biodegradation, 65*(6), 757–767.
79. Yao, Z., Seong, H. J., & Jang, Y. S. (2022). Degradation of low density polyethylene by *Bacillus* species. *Applied Biological Chemistry, 65*(1), 1–9.
80. Sivan, A., Szanto, M., & Pavlov, V. (2006). Biofilm development of the polyethylene-degrading bacterium *Rhodococcus ruber*. *Applied Microbiology and Biotechnology, 72*, 346–352.
81. Jayan, N., Skariyachan, S., & Sebastian, D. (2023). The escalated potential of the novel isolate *Bacillus cereus* NJD1 for effective biodegradation of LDPE films without pre-treatment. *Journal of Hazardous Materials, 455*, 131623.
82. Liu, R., Zhao, S., Zhang, B., Li, G., Fu, X., Yan, P., & Shao, Z. (2023). Biodegradation of polystyrene (PS) by marine bacteria in mangrove ecosystem. *Journal of Hazardous Materials, 442*, 130056.
83. Gupta, K. K., Sharma, K. K., & Chandra, H. (2023). Utilization of *Bacillus cereus* strain CGK5 associated with cow feces in the degradation of commercially available high-density polyethylene (HDPE). *Archives of Microbiology, 205*(3), 101.
84. Nyamjav, I., Jang, Y., Lee, Y. E., & Lee, S. (2023). Biodegradation of polyvinyl chloride by *Citrobacter koseri* isolated from superworms (*Zophobas atratus* larvae). *Frontiers in Microbiology, 14*, 1175249.
85. Xu, A., Zhou, J., Blank, L. M., & Jiang, M. (2023). Future focuses of enzymatic plastic degradation. *Trends in Microbiology, 31*(7), 668–671.
86. Schmidt, J., Wei, R., Oeser, T., Dedavid e Silva, L. A., Breite, D., Schulze, A., & Zimmermann, W. (2017). Degradation of polyester polyurethane by bacterial polyester hydrolases. *Polymers, 9*(2), 65.
87. Furukawa, M., Kawakami, N., Tomizawa, A., & Miyamoto, K. (2019). Efficient degradation of poly (ethylene terephthalate) with *Thermobifida fusca* cutinase exhibiting improved catalytic activity generated using mutagenesis and additive-based approaches. *Science and Reports, 9*(1), 16038.
88. Blázquez-Sánchez, P., Engelberger, F., Cifuentes-Anticevic, J., Sonnendecker, C., Griñén, A., Reyes, J., Díez, B., Guixé, V., Richter, P. K., Zimmermann, V., & Ramírez-Sarmiento, C. A. (2022). Antarctic polyester hydrolases degrade aliphatic and aromatic polyesters at moderate temperatures. *Applied and Environment Microbiology, 88*(1), e01842-21.
89. Sonnendecker, C., Oeser, J., Richter, P. K., Hille, P., Zhao, Z., Fischer, C., Lippold, H., Blázquez-Sánchez, P., Engelberger, F., Ramírez-Sarmiento, C. A., Oeser, T., Lihanova, Y., Frank, R., Jahnke, H. G., Billig, S., Abel, B., Sträter, N., Matysik, J., & Zimmermann, W. (2022). Low carbon footprint recycling of post-consumer PET plastic with a metagenomic polyester hydrolase. *Chemsuschem, 15*(9), e202101062.
90. Zhang, H., Dierkes, R. F., Perez-Garcia, P., Costanzi, E., Dittrich, J., Cea, P. A., Gurschke, M., Applegate, V., Partus, K., Schmeisser, C., Pfleger, C., Gohlke, H., Smits, S. H. J., Chow, J., & Streit, W. R. (2023). The metagenome-derived esterase PET40 is highly promiscuous and hydrolyses polyethylene terephthalate (PET). *The FEBS Journal*. https://doi.org/10.1111/febs.16924
91. Herbert, J., Beckett, A. H., & Robson, S. C. (2022). A review of cross-disciplinary approaches for the identification of novel industrially relevant plastic-degrading enzymes. *Sustainability, 14*(23), 15898.
92. Shahnawaz, M., Sangale, M. K., & Ade, A. B. (2016). Bacteria-based polythene degradation products: GC-MS analysis and toxicity testing. *Environmental Science and Pollution Research, 23*, 10733–10741.
93. Khandare, S. D., Chaudhary, D. R., & Jha, B. (2022). Marine bacteria-based polyvinyl chloride (PVC) degradation by-products: Toxicity analysis on *Vigna radiata* and edible seaweed *Ulva lactuca*. *Marine Pollution Bulletin, 175*, 113366.
94. Peng, B. Y., Chen, Z., Chen, J., Yu, H., Zhou, X., Criddle, C. S., Wu, W. M., & Zhang, Y. (2020). Biodegradation of polyvinyl chloride (PVC) in *Tenebrio molitor* (Coleoptera: Tenebrionidae) larvae. *Environment International, 145*, 106106.